



Quest for a comprehensive shell model to track the evolution in nuclear structure

Rebeka Sultana Lubna

Facility for Rare Isotope Beams (FRIB)



MICHIGAN STATE
UNIVERSITY

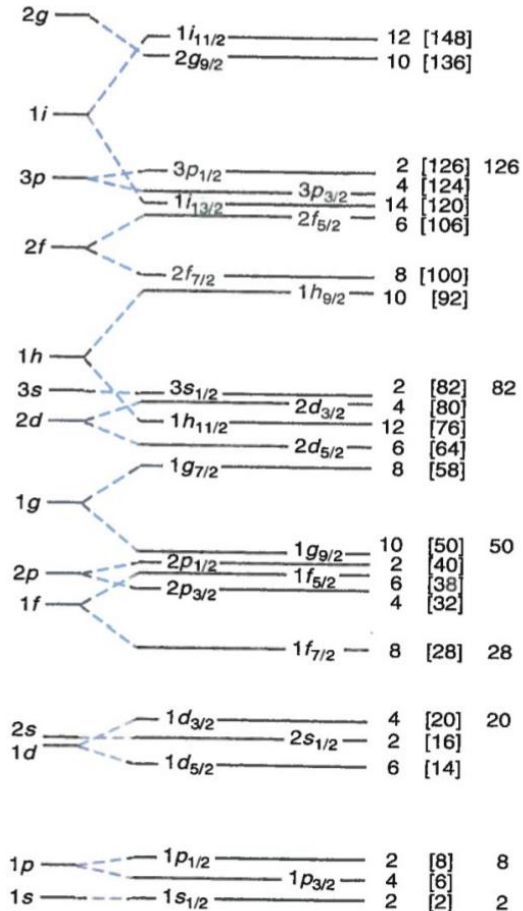


U.S. DEPARTMENT OF
ENERGY

Office of
Science

This material is based upon work supported by the U.S. Department of Energy, Office of Science, Office of Nuclear Physics and used resources of the Facility for Rare Isotope Beams (FRIB) Operations, which is a DOE Office of Science User Facility under Award Number DE-SC0023633.

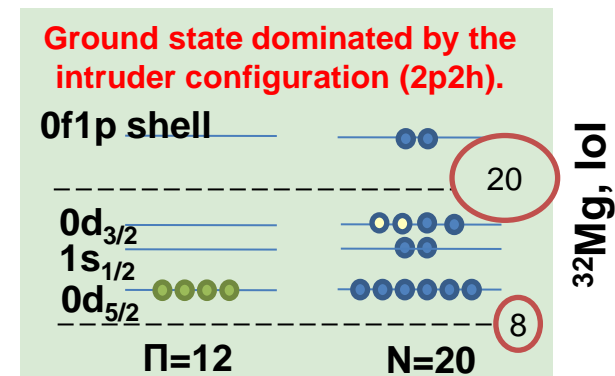
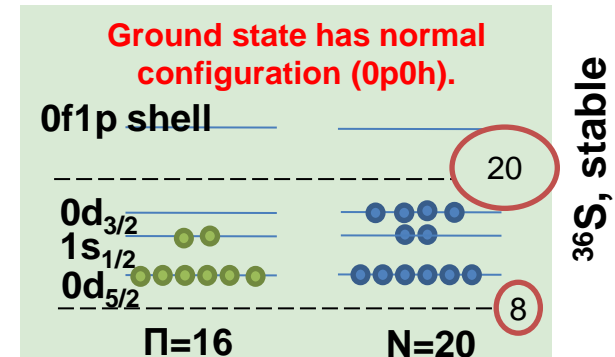
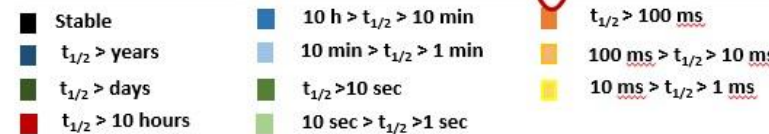
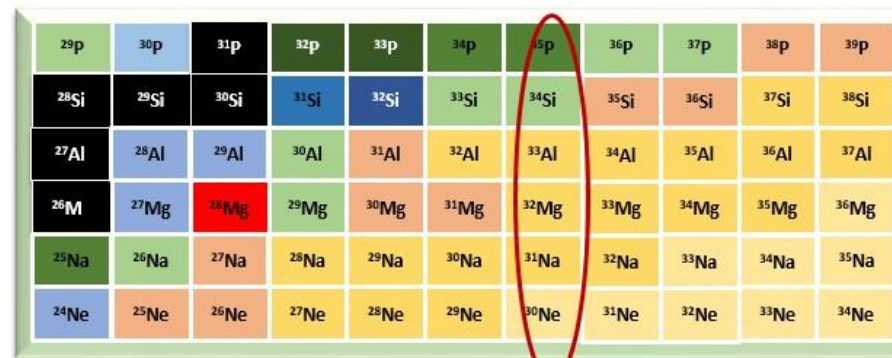
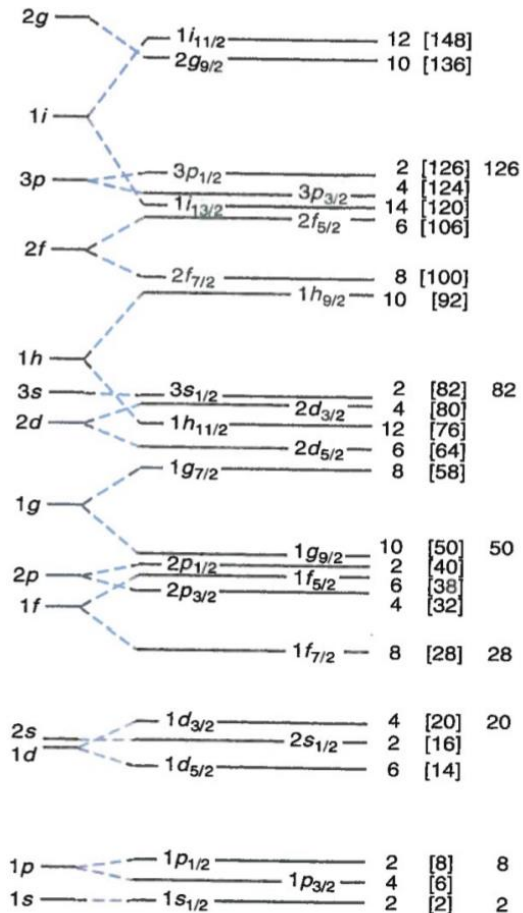
Evolution of Nuclear Shell Structure



- Nuclear shell gaps and hence the magic numbers are not constant as they were believed to be.
- Nuclei with high N/Z → Normal magic number disappear; new magic number can emerge.

Evolution of Nuclear Shell Structure

- Nuclear shell gaps and hence the magic numbers are not constant as they were believed to be.
- Nuclei with high N/Z → Normal magic number disappear; new magic number can emerge.
- Disappearance effect of the neutron magic number 20 in the nuclei within the Island of Inversion (IoI).



Evolution of Nuclear Shell Structure

Highlighted region $Z \leq 20$, $N \geq 20$

<http://www.nuclear.csdb.cn/nuclear/index.asp>

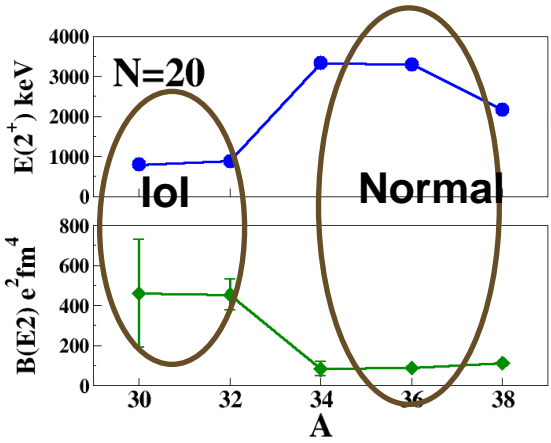
20	Ca37 181.1 MS	Ca38 440 MS	Ca39 890.6 MS	Ca40 96.94	Ca41 109000 Y	Ca42 0.647	Ca43 0.135	Ca44 2.09	Ca45 162.61 D	Ca46 0.004	Ca47 4.536 D	Ca48 0.187	Ca49 8.718 M	Ca50 13.9 S	Ca51 100 S	Ca52 4.6 S
19	K36 342 MS	K37 1.226 S	K38 7.636 M	K39 93.2981	K40 0.0117	K41 6.7302	K42 12.360 H	K43 22.3 H	K44 22.13 M	K45 17.3 M	K46 105 S	K47 17.50 S	K48 6.8 S	K49 1.26 S	K50 472 MS	K51 365 MS
18	Ar35 1.775 S	Ar36 0.3365	Ar37 3504 D	Ar38 0.0632	Ar39 260 Y	Ar40 99.6005	Ar41 10934 M	Ar42 32.9 Y	Ar43 5.37 M	Ar44 11.87 M	Ar45 21.48 S	Ar46 8.4 S	Ar47 ~700 MS	Ar48	Ar49 ~170 NS	Ar50 ~170 NS
17	Cl34 1.5264 S	Cl35 75.77	Cl36 301000 Y	Cl37 24.23	Cl38 37.24 M	Cl39 55.6 M	Cl40 1.35 M	Cl41 38.4 S	Cl42 6.8 S	Cl43 3.3 S	Cl44 0.56 S	Cl45 400 MS	Cl46 223 MS	Cl47 >200 NS	Cl48 >200 NS	Cl49 ~170 NS
16	S33 0.75	S34 4.21	S35 87.38 D	S36 0.02	S37 5.05 M	S38 170.3 M	S39 11.5 S	S40 8.8 S	S41 2.6 S	S42 0.56 S	S43 220 MS	S44 123 MS	S45 82 MS	S46 >200 NS	S47 >200 NS	S48 >200 NS
15	P32 14.262 D	P33 25.34 D	P34 12.43 S	P35 47.3 S	P36 5.6 S	P37 2.31 S	P38 0.64 S	P39 0.16 S	P40 260 MS	P41 120 MS	P42 110 MS	P43 33 MS	P44 >200 NS	P45 >200 NS	P46 >200 NS	
14	Si31 1.573 M	Si32 1.72 Y	Si33 6.332 S	Si34 2.77 S	Si35 0.78 S	Si36 0.45 S	Si37 90 MS	Si38 >1 US	Si39 >1 US	Si40 >200 NS	Si41 >200 NS	Si42 >200 NS				
13	Al30 3.60 S	Al31 644 MS	Al32 33 MS	Al33 >1 US	Al34 60 MS	Al35 1.50 MS	Al36 90 MS	Al37	Al38 >200 NS	Al39 >200 NS	Al40 >260 NS	28				
12	Mg29 1.30 S	Mg30 335 MS	Mg31 230 MS	Mg32 120 MS	Mg33 90 MS	Mg34 20 MS	Mg35 70 MS	Mg36 >200 NS	Mg37 >260 NS							
11	Na28 30.5 MS	Na29 44.9 MS	Na30 48 MS	Na31 170 MS	Na32 132 MS	Na33 82 MS	Na34 5.5 MS	Na35 1.5 MS								
10	Ne27 32 MS	Ne28 17 MS	Ne29 200 MS	Ne30 >200 NS	Ne31 >260 NS	Ne32 >200 NS										

- Evolution of shell structure in light neutron-rich systems led to the discoveries in dramatic changes in magic numbers.
- Studies conducted near $N = 20$, huge prospects close to $N = 28$ with the radioactive ion beam.

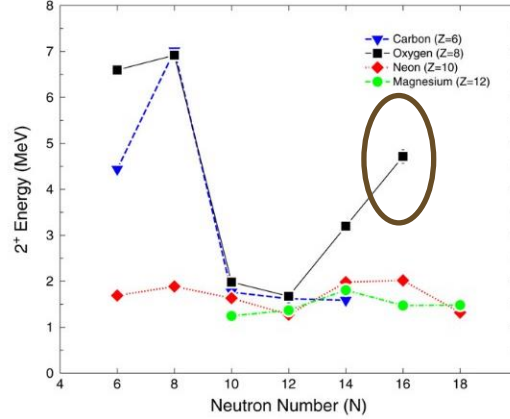


Experimental Signatures of Structural Evolution

2^+_1 state and $B(E2:0^+ \rightarrow 2^+)$



- Island of inversion
- Low-lying 2^+_1 level, high $B(E2)$
- New magic number High 2^+_1



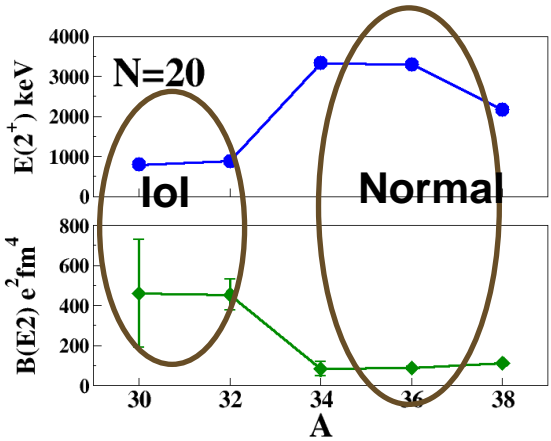
C.R. Hoffman *et al.*, Physics Letters B 672 17 (2009)



Experimental Signatures of Structural Evolution

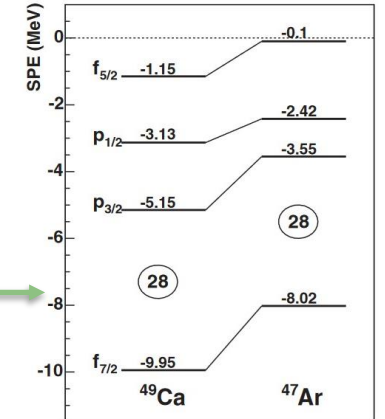
2^+_1 state and $B(E2:0^+ \rightarrow 2^+)$

Single-particle properties

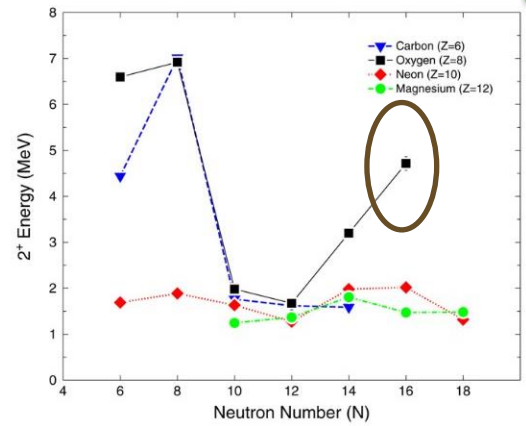


- Island of inversion
- Low-lying 2^+_1 level, high $B(E2)$
- New magic number High 2^+_1

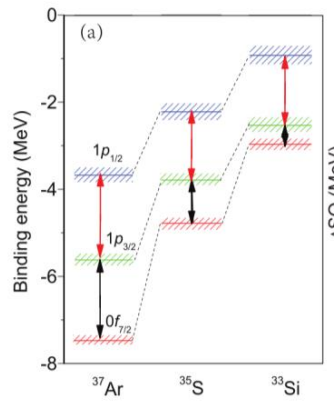
SPE: Orbitals' locations, probe shell gap



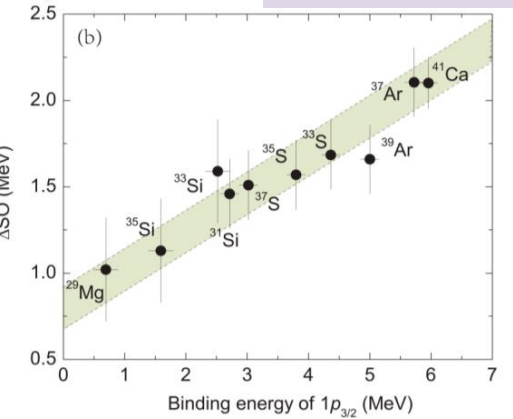
L. Gaudfrey *et al.*, Phys. Rev. Lett. 97, 092501 (2006)



C.R. Hoffman *et al.*, Physics Letters B 672 17 (2009)

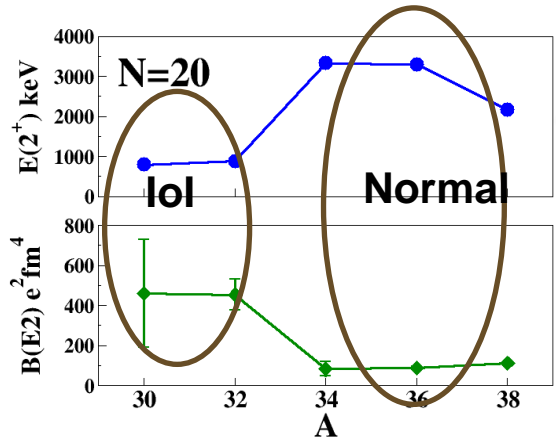


J. Chen *et al.*, Phys. Lett. B 835, 138678 (2024)



Experimental Signatures of Structural Evolution

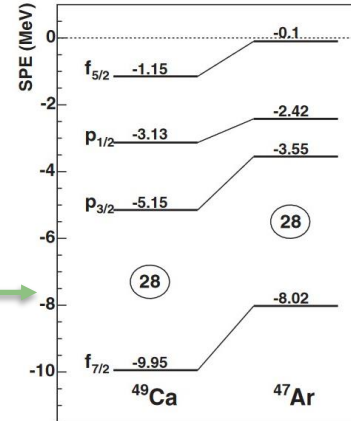
2^+_1 state and $B(E2:0^+ \rightarrow 2^+)$



- Island of inversion
- Low-lying 2^+_1 level, high $B(E2)$
- New magic number High 2^+_1

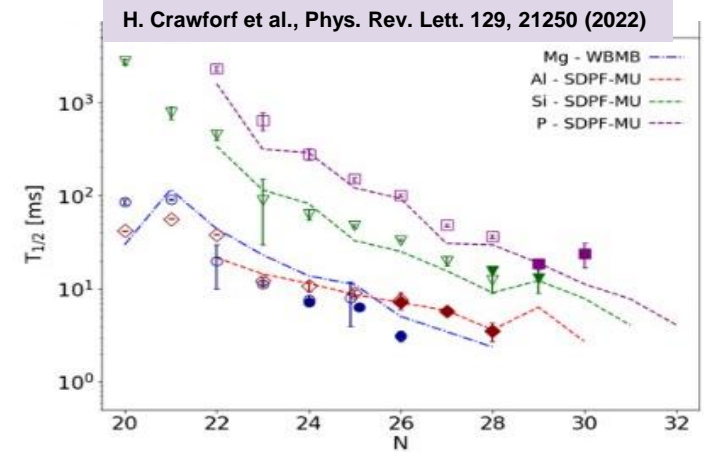
SPE: Orbitals' locations, probe shell gap

Single-particle properties



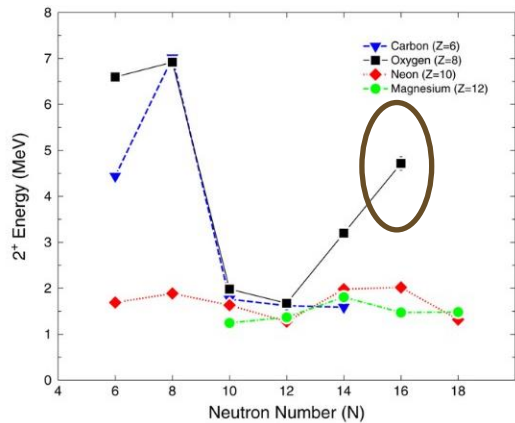
L. Gaudetroy *et al.*, Phys. Rev. Lett. 97, 092501 (2006)

Ground-state half-life

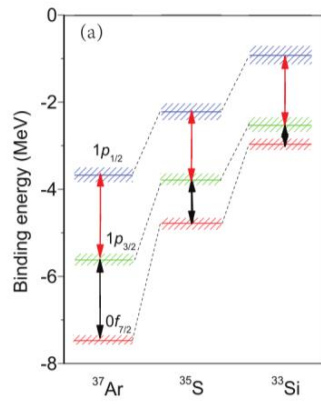


H. Crawford *et al.*, Phys. Rev. Lett. 129, 21250 (2022)

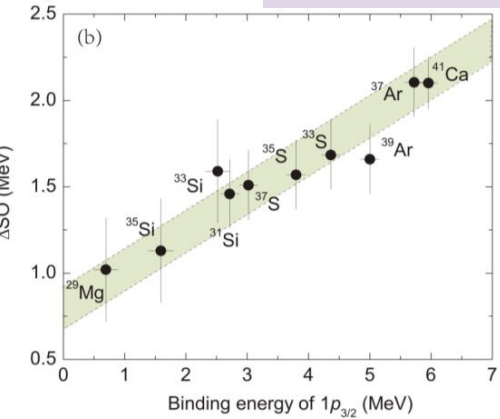
V. Tripathi *et al.*, Phys. Rev. C 106, 064314 (2022)



C.R. Hoffman *et al.*, Physics Letters B 672 17 (2009)

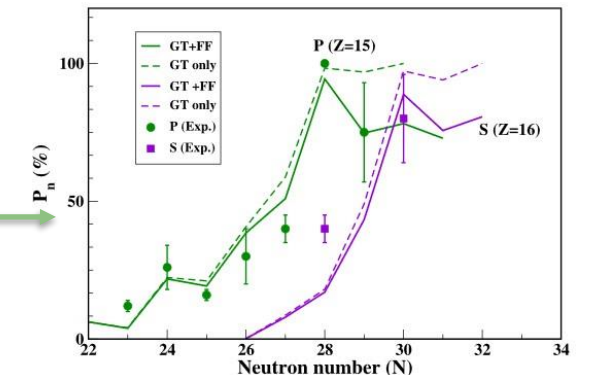


J. Chen *et al.*, Phys. Lett. B 835, 138678 (2024)



Exotic phenomena in decay properties at heightened N/Z

Neutron emission probability



Data-driven Shell-model interactions and modifications

WBP¹ → WBP-a²

- Adjusted single-particle energies (SPE) of $0f_{7/2}$ and $1p_{3/2}$ orbitals to better reproduce energy states of even-mass P isotopes.
- Reduced single particle energies (SPE) of $0f_{7/2}$ by 1.8 MeV and $1p_{3/2}$ by 0.5 MeV.
- Provided satisfactory prediction of the negative-parity energy levels.

WBP	EXP	WBP-a	WBP	EXP	WBP-a	WBP	EXP	WBP-a
				6192 ⁻ 6 ⁻	6115 ⁻ 6 ⁻	3902 ⁻ 4 ⁻		
			5978 ⁻ 6 ⁻		5710 ⁻ 6 ⁻	3576 ⁻ 5 ⁻		
						3562 ⁻ 3 ⁻		
						3337 ⁻ 1 ⁻		
						3137 ⁻ 0 ⁻		
						3113 ⁻ 2 ⁻		
			5002 ⁻ 6 ⁻		4887 ⁻ 5 ⁻			
				4629 ⁻ 6 ⁻	4792 ⁻ 6 ⁻			2390 ⁻ 5 ⁻
			4286 ⁻ 5 ⁻					2079 ⁻ 2 ⁻
						4084 ⁻ 5 ⁻		
4995 ⁻ 4 ⁻		5155 ⁻ 4 ⁻	3823 ⁻ 5 ⁻	3950 ⁻ 5 ⁻	3881 ⁻ 3 ⁻			
	4849 ⁻ (4 ⁻)	5137 ⁻ 0 ⁻			3707 ⁻ 4 ⁻			
4691 ⁻ 3 ⁻	4661 ⁻ 2 ⁻	4882 ⁻ 3 ⁻	3399 ⁻ 3 ⁻	3352 ⁻ 5 ⁻	3576 ⁻ 5 ⁻	1307 ⁻ 4 ⁻		
4595 ⁻ 5 ⁻	4409 ⁻ 0 ⁻	4567 ⁻ 2 ⁻	3191 ⁻ 4 ⁻			1297 ⁻ 3 ⁻		
	4275 ⁻ 5 ⁻	4407 ⁻ 5 ⁻						
	4149 ⁻ 3 ⁻							
	4036 ⁻ 1 ⁻							
	4009 ⁻ 2 ⁻	3980 ⁻ 1 ⁻			2887 ⁻ 1 ⁻	627 ⁻ 1 ⁻		669 ⁻ 1 ⁻
3586 ⁻ 4 ⁻			2435 ⁻ 4 ⁻	2320 ⁻ 3 ⁻	2294 ⁻ 2 ⁻		250 ⁻ (2 ⁻ , 3 ⁻)	235 ⁻ 3 ⁻
3291 ⁻ 3 ⁻	3443 ⁻ 4 ⁻	3432 ⁻ 4 ⁻	2278 ⁻ 3 ⁻	2305 ⁻ 4 ⁻	2249 ⁻ 4 ⁻	0 ⁻ 2 ⁻	0 ⁻ 4 ⁻	113 ⁻ 4 ⁻
3205 ⁻ 1 ⁻	3320 ⁻ 3 ⁻	3375 ⁻ 2 ⁻	2033 ⁻ 1 ⁻		2175 ⁻ 3 ⁻			0 ⁻ 2 ⁻
	3264 ⁻ 2 ⁻	3279 ⁻ 3 ⁻						
	32P							
2274 ⁻ 2 ⁻			1555 ⁻ 2 ⁻	34P				36P



Data-driven Shell-model interactions and modifications

WBP¹ → WBP-b²

- Adjusted single-particle energies (SPE) of $0f_{7/2}$ and $1p_{1/2}$ orbitals to better reproduce energy states of odd-mass Si isotopes.
- Reduced SPE of $0f_{7/2}$ by 1.4 MeV and raised $1p_{1/2}$ by 0.4 MeV.
- Provided satisfactory interpretation of the negative-parity intruder energy levels.

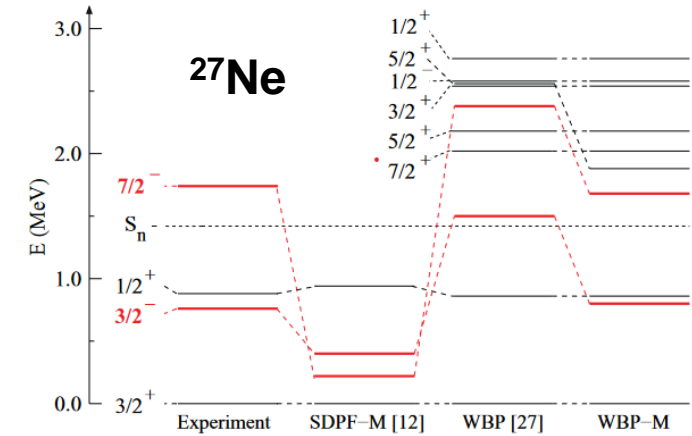
	<u>6781</u> 11/2	<u>6855</u> 11/2			
		<u>5547</u> 9/2			
	<u>5254</u> 9/2		<u>5311</u> 11/2	<u>5375</u> 11/2	
	<u>4934</u> 3/2	<u>4818</u> 3/2	<u>4998</u> 9/2	<u>5121</u> 9/2	Exp. WBP-b
		<u>3887</u> 7/2			<u>4433</u> 11/2
	<u>3623</u> 7/2		<u>3533</u> 3/2	<u>3524</u> 3/2	<u>4090</u> 11/2
	Exp.	WBP-b	<u>3134</u> 7/2	<u>2922</u> 7/2	<u>3497</u> 9/2
					<u>3159</u> 9/2
			Exp.	WBP-b	<u>2295</u> 3/2
					<u>1981</u> 3/2
					<u>1435</u> 7/2
					<u>1629</u> 7/2



Data-driven Shell-model interactions and modifications

$$\text{WBP}^1 \longrightarrow \text{WBP-M}^2$$

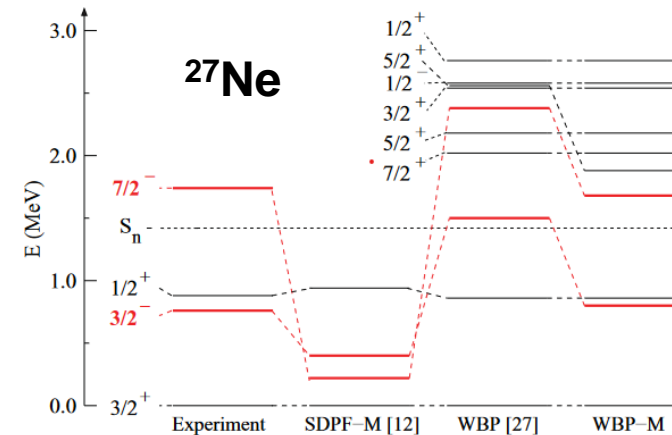
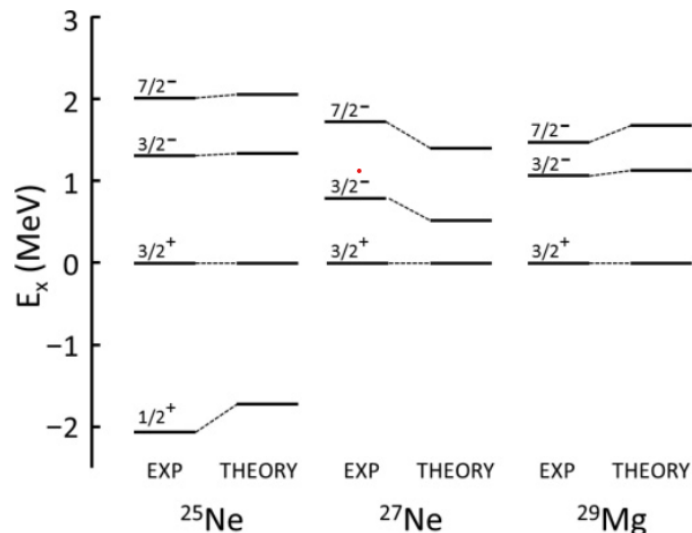
- Adjusted single-particle energies (SPE) of fp-shell orbitals to better reproduce energy states of ^{27}Ne .
- Reduced SPE of 0f-1p shell orbitals by 0.7 MeV.
- For the nearby isotopes, it required 1.0 MeV reduction.



Data-driven Shell-model interactions and modifications

WBP¹ → WBP-M²

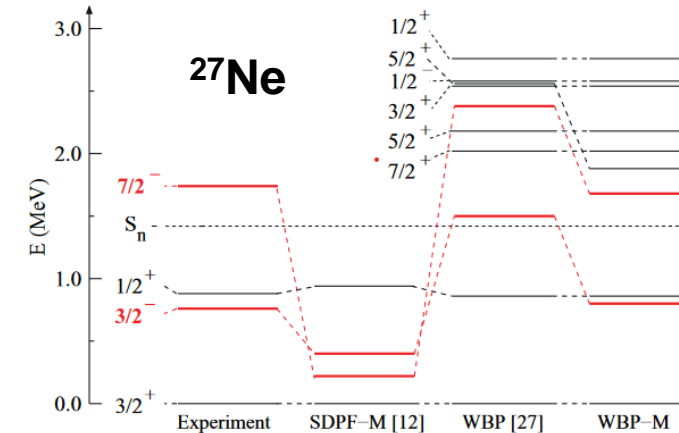
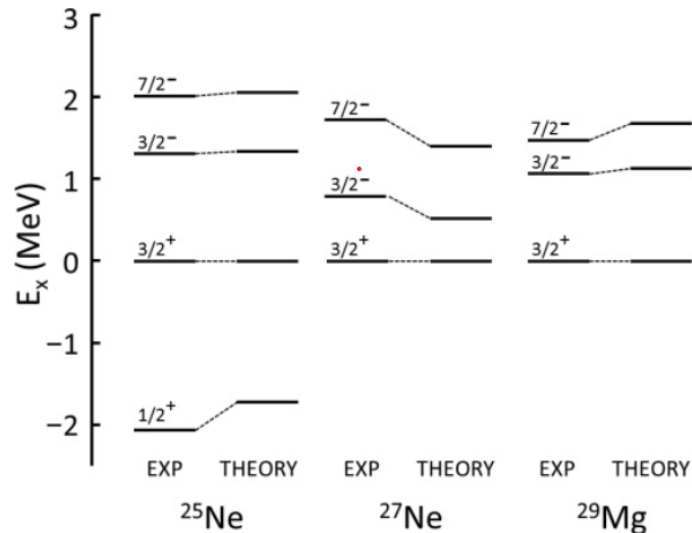
- Adjusted single-particle energies (SPE) of fp-shell orbitals to better reproduce energy states of ²⁷Ne.
- Reduced SPE of 0f-1p shell orbitals by 0.7 MeV.
- For the nearby isotopes, it required 1.0 MeV reduction.



Data-driven Shell-model interactions and modifications

WBP¹ → WBP-M²

- Adjusted single-particle energies (SPE) of fp-shell orbitals to better reproduce energy states of ²⁷Ne.
- Reduced SPE of 0f-1p shell orbitals by 0.7 MeV.
- For the nearby isotopes, it required 1.0 MeV reduction.



PHYSICAL REVIEW C 85, 011302(R) (2012)

Low-lying neutron fp-shell intruder states in ²⁷Ne

S. M. Brown,¹ W. N. Catford,¹ J. S. Thomas,¹ B. Fernández-Domínguez,^{2,3} N. A. Orr,² M. Labiche,⁴ M. Rejmund,⁵ N. L. Achouri,² H. Al Falou,² N. I. Ashwood,⁶ D. Beaumel,⁷ Y. Blumenfeld,⁷ B. A. Brown,⁸ R. Chapman,⁹ M. Chartier,³ N. Curtis,⁶ G. de France,⁵ N. de Sereville,⁷ F. Delaunay,² A. Drouart,¹⁰ C. Force,⁵ S. Franchoo,⁷ J. Guillot,⁷ P. Haigh,⁶ F. Hammache,⁷ V. Lapoux,¹⁰ R. C. Lemmon,⁴ A. Leprince,⁷ F. Maréchal,⁷ X. Mougeot,¹⁰ B. Mougnot,⁷ L. Nalpas,¹⁰ A. Navin,³ N. P. Patterson,¹ B. Pietras,³ E. C. Pollacco,¹⁰ A. Ramus,⁷ J. A. Scarpaci,⁷ I. Stefan,⁷ and G. L. Wilson¹

¹Faculty of Engineering and Physical Sciences, University of Surrey, Guildford, GU2 7XH, UK
²LPC-Caen, ENSICAEN, Université de Caen, CNRS/IN2P3, F-14050 Caen Cedex, France
³Oliver Lodge Laboratory, School of Physical Sciences, University of Liverpool, Liverpool L69 7ZE, UK
⁴Nuclear Structure Group, STFC Daresbury Laboratory, Daresbury, Warrington WA4 4AD, UK
⁵GANIL, BP 55027, F-14076 Caen Cedex 5, France
⁶School of Physics and Astronomy, University of Birmingham, Birmingham B15 2TT, UK
⁷IPN-Orsay, F-91406 Orsay, France
⁸NSCL and Department of Physics and Astronomy, Michigan State University, East Lansing, Michigan 48824, USA
⁹SUPA, School of Engineering, University of the West of Scotland, Paisley PA1 2BE, UK
¹⁰CEA-Saclay, IRFU/Service de Physique Nucléaire, F-91191 Gif-sur-Yvette, France

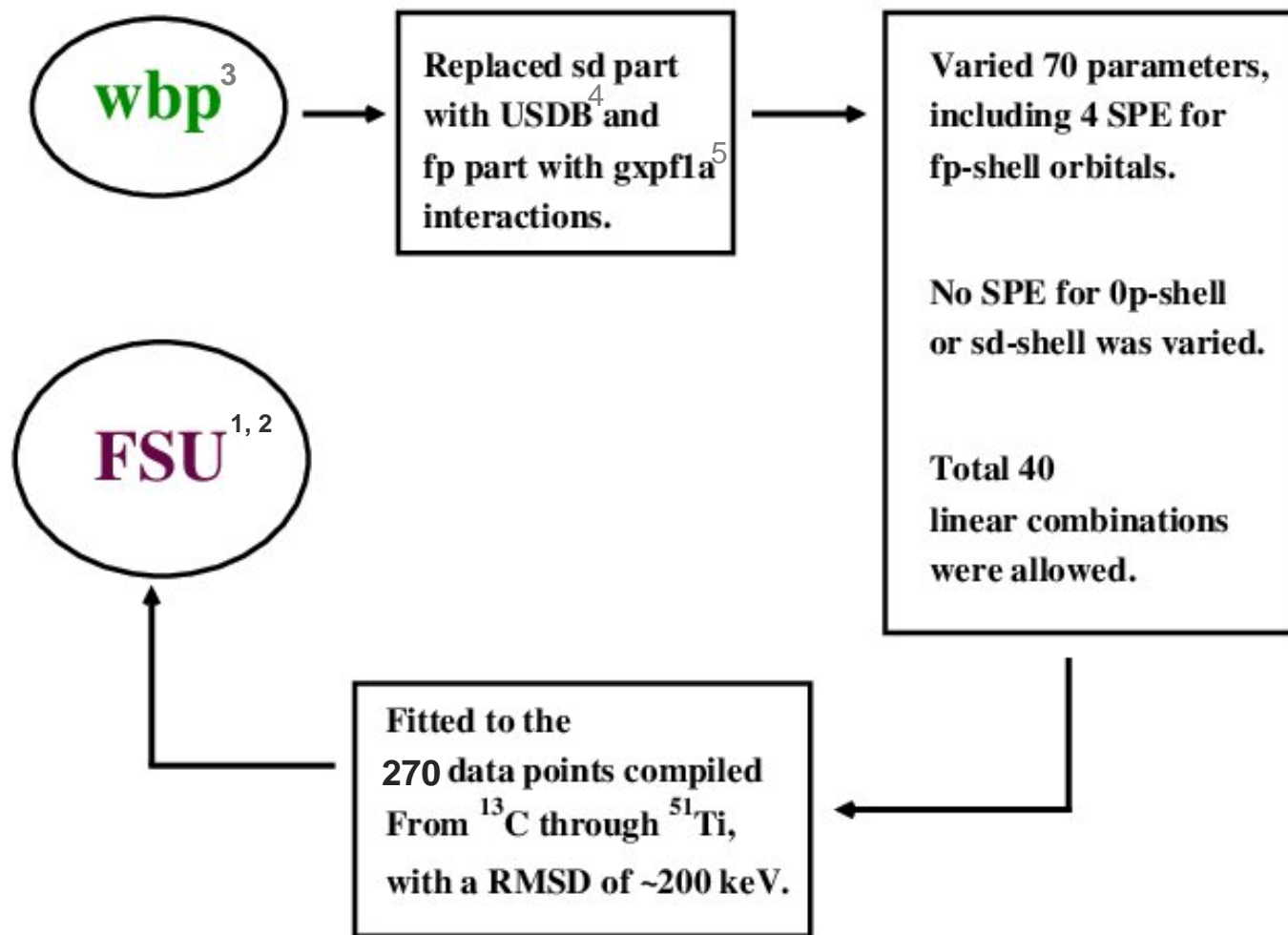
(Received 7 April 2011; published 23 January 2012)

It would be interesting to develop a new interaction that would succeed in reducing the effective gap between the $0d_{3/2}$ orbital and the $0f-1p$ shell in a natural way, without the need for *ad hoc* changes.



1. E. K. Warburton and B. A. Brown, Phys. Rev. C 46, 923 (1992).
 2. S.M.Brown *et al.*, Phys. Rev. C 85, 011302(R) (2012).

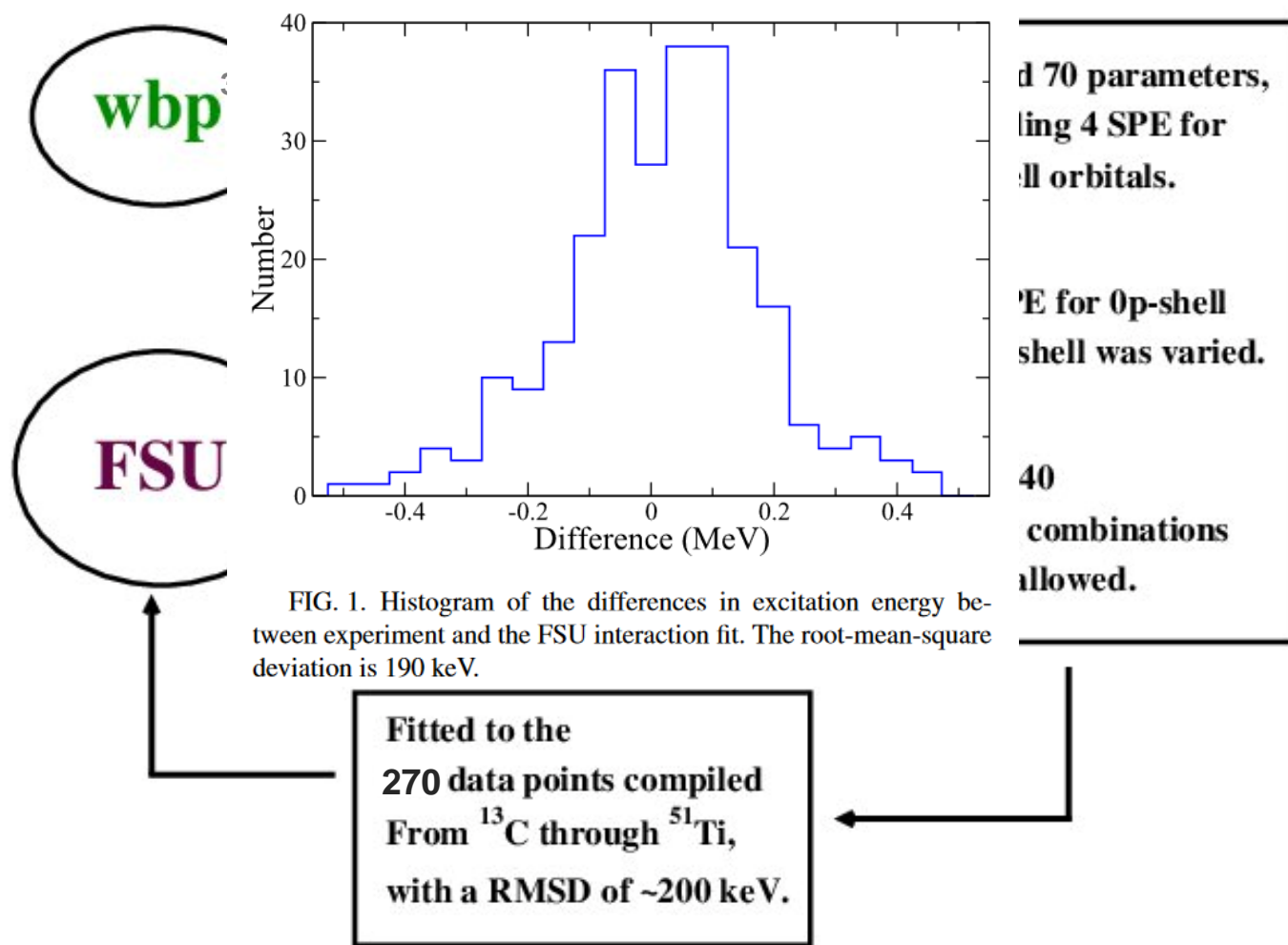
Quest for a Comprehensive Shell-Model Interaction



- Empirical shell-model interaction FSU^{1,2} was developed within *spsd-fp* model-space using data fitting procedure.
- A modified version of the WBP³ interaction was used as the starting point.
- sd-shell TBME replaced with USDB.⁴
- Fp-shell TBME replaced with gxpfla.⁵
- Data fitting was performed within the *p-sd-fp* model-space.
- A linear combination of 70 parameters were fitted by using 270 experimentally observed states compiled from the NNDC.⁶

1. R. S. Lubna *et al.*, *Phys. Rev. C* 100, 034308 (2019)
2. R. S. Lubna *et al.*, *Phys. Rev. Research* 2, 043342 (2020)
3. E. K. Warburton and B. A. Brown, *Phys. Rev. C* 46, 923 (1992).
4. B. A. Brown and W. A. Richter, *Phys. Rev. C* 74, 034315 (2006).
5. M. Homa *et al.*, *Eur. Phys. J A* 25, 499 (2005).
6. www.nndc.bnl.gov

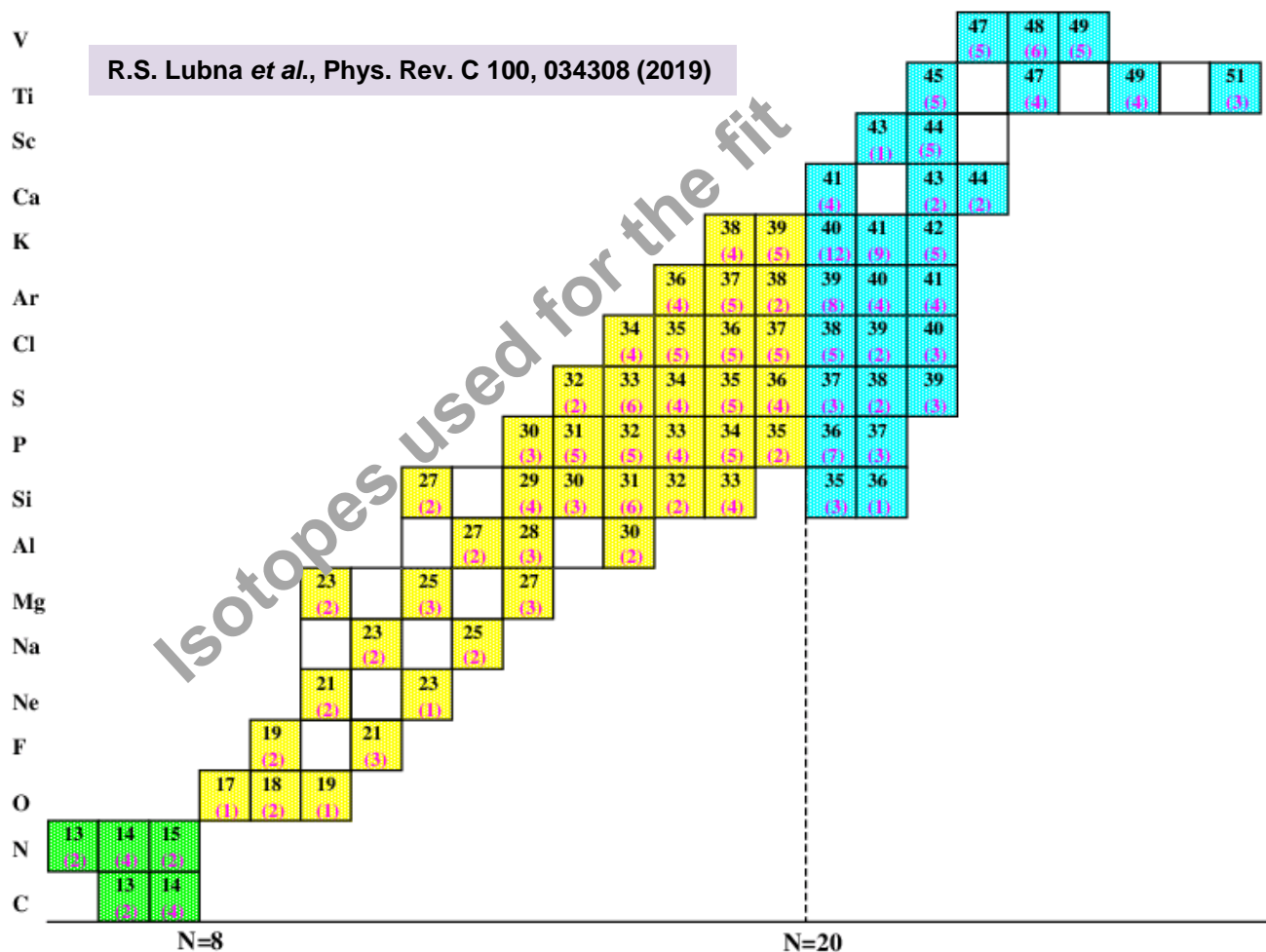
Quest for a Comprehensive Shell-Model Interaction



- Empirical shell-model interaction FSU^{1,2} was developed within *spstdfp* model-space using data fitting procedure.
- A modified version of the WBP³ interaction was used as the starting point.
- sd-shell TBME replaced with USDB.⁴
- Fp-shell TBME replaced with gxp1a.⁵
- Data fitting was performed within the *p-sd-fp* model-space.
- A linear combination of 70 parameters were fitted by using 270 experimentally observed states compiled from the NNDC.⁶

1. R. S. Lubna *et al.*, *Phys. Rev. C* 100, 034308 (2019)
2. R. S. Lubna *et al.*, *Phys. Rev. Research* 2, 043342 (2020)
3. E. K. Warburton and B. A. Brown, *Phys. Rev. C* 46, 923 (1992).
4. B. A. Brown and W. A. Richter, *Phys. Rev. C* 74, 034315 (2006).
5. M. Homa *et al.*, *Eur. Phys. J A* 25, 499 (2005).
6. www.nndc.bnl.gov

Quest for a Comprehensive Shell-Model Interaction

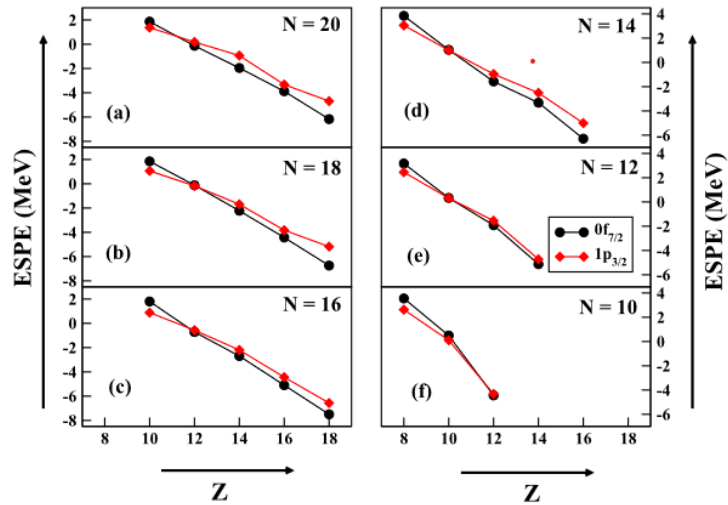


- Empirical shell-model interaction FSU^{1,2} was developed within *spdfp* model-space using data fitting procedure.
- A modified version of the WBP³ interaction was used as the starting point.
- *sd*-shell TBME replaced with USDB.⁴
- *Fp*-shell TBME replaced with *gxp1a*.⁵
- Data fitting was performed within the *p-sd-fp* model-space.
- A linear combination of 70 parameters were fitted by using 270 experimentally observed states compiled from the NNDC.⁶

1. R. S. Lubna *et al.*, Phys. Rev. C 100, 034308 (2019)
2. R. S. Lubna *et al.*, Phys. Rev. Research 2, 043342 (2020)
3. E. K. Warburton and B. A. Brown, Phys. Rev. C 46, 923 (1992).
4. B. A. Brown and W. A. Richter, Phys. Rev. C 74, 034315 (2006).
5. M. Homa *et al.*, Eur. Phys. J A 25, 499 (2005).
6. www.nndc.bnl.gov

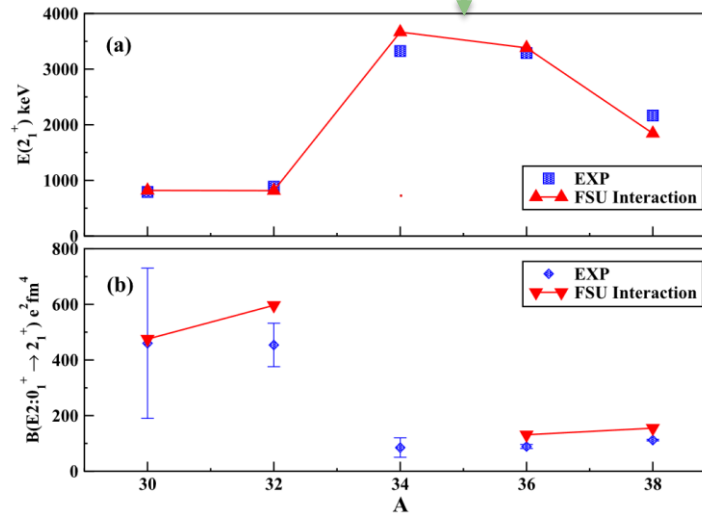
Quest for a Comprehensive Shell-Model Interaction

R. S. Lubna et al., *Phys. Rev. Research* 2, 043342 (2020)



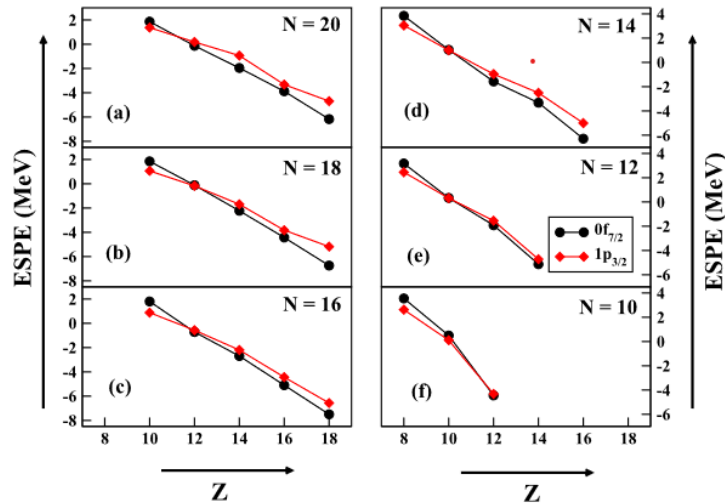
Crossing between $0f_{7/2}$ and $1p_{3/2}$ occurs between $Z=10$ and 12 , suggesting that the $N=28$ shell gap shifts to $N=24$ with lower Z .

Experimental $E(2^+)$ and $B(E2)$ values for the $N=20$ isotones compared to the predictions



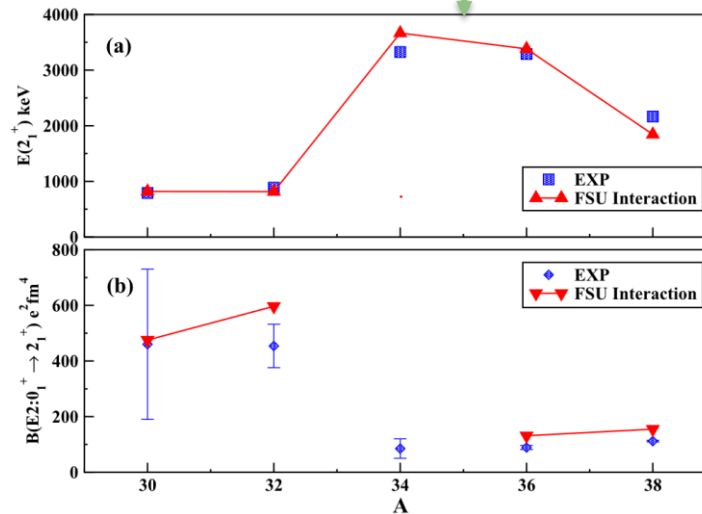
Quest for a Comprehensive Shell-Model Interaction

R. S. Lubna et al., Phys. Rev. Research 2, 043342 (2020)

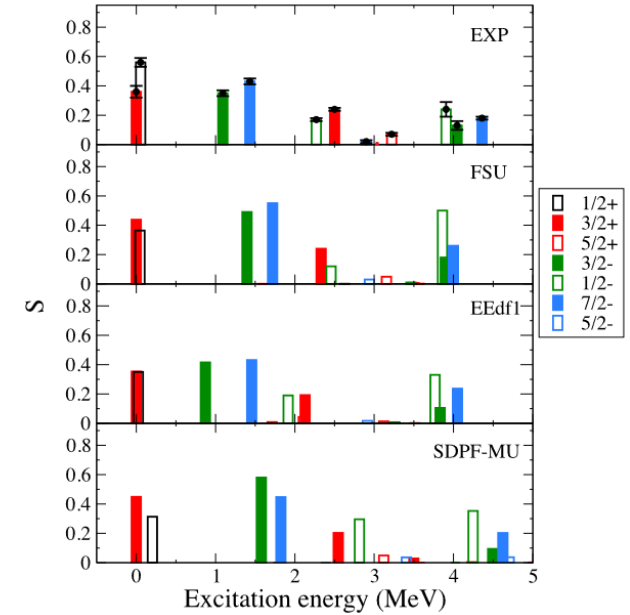


Crossing between $0f_{7/2}$ and $1p_{3/2}$ occurs between $Z=10$ and 12 , suggesting that the $N=28$ shell gap shifts to $N=24$ with lower Z .

Experimental $E(2^+)$ and $B(E2)$ values for the $N=20$ isotones compared to the predictions



P.T. MacGregor et al., Phys. Rev. C 104, L051301 (2021)



- States populated in ^{29}Mg via (d, p) reaction.
- Opposite-parity states provide test to the models.

Are we there yet?

- Do we have a comprehensive model for the *s-p-sd-pf* model space?
- Short answer is “Not yet”
- Major limitations lies in predicting structural properties for
 - Higher ratio of N/Z.
 - Mid-shell nuclei.
 - Opposite-parity intruder states.
 - And many more...
- Require ‘useful’ data from experiments.



β^- Decay in Exploring Shell Evolution

β^- decay grants access to very exotic isotopes

β xn branches:

- Understand the process of β -delayed neutron emission.

β -delayed γ transitions:

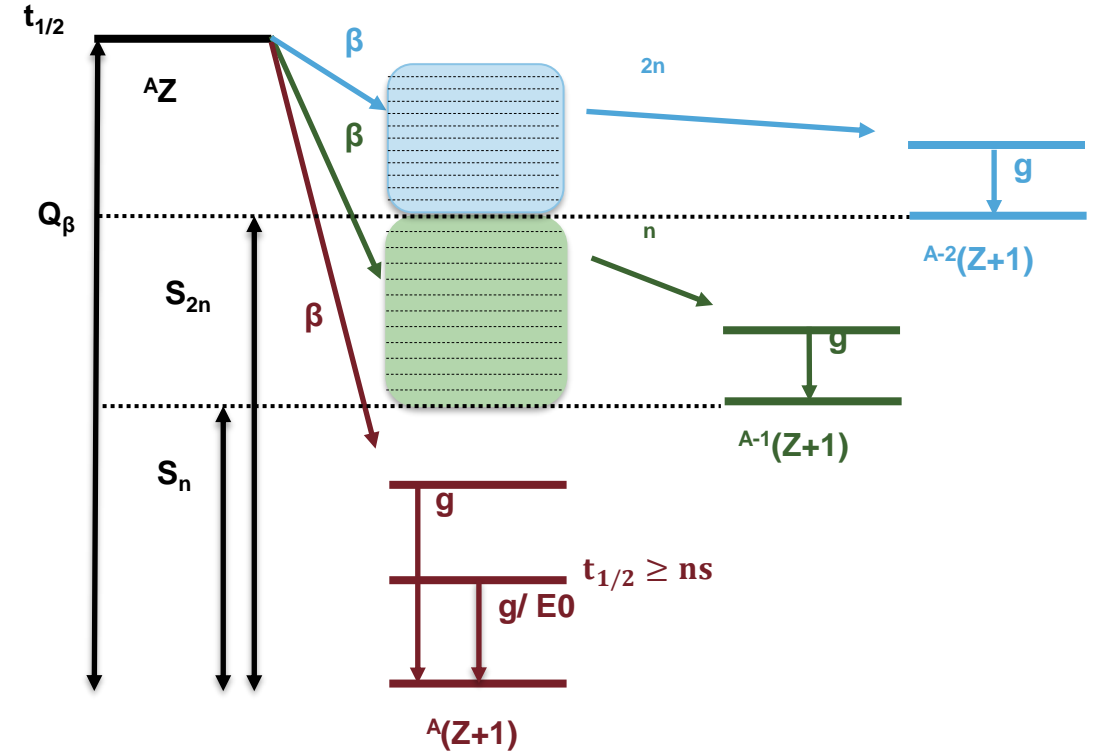
- Level structure of the descendant nuclei.
- GT and FF transition strength.

Ground-state half-life:

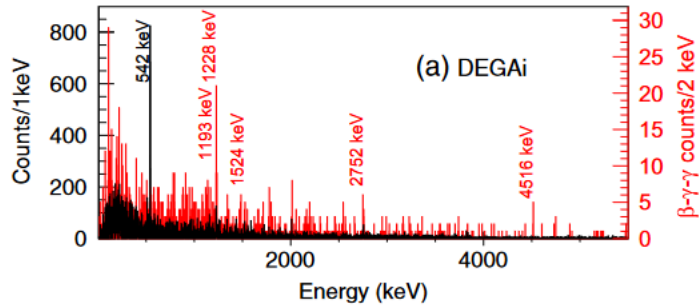
- First insight into the structure.
- Shell-structure and evolution.

Isomers and Shape co-existence:

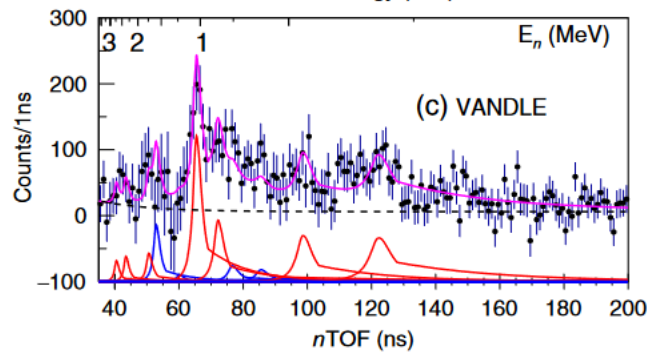
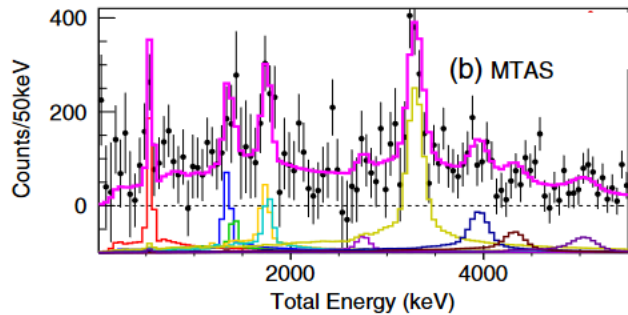
- β -decay can populate isomers.
- Can decay via β , γ or IC/ IPF.
- Provide Insight into shape/ configuration coexistence.



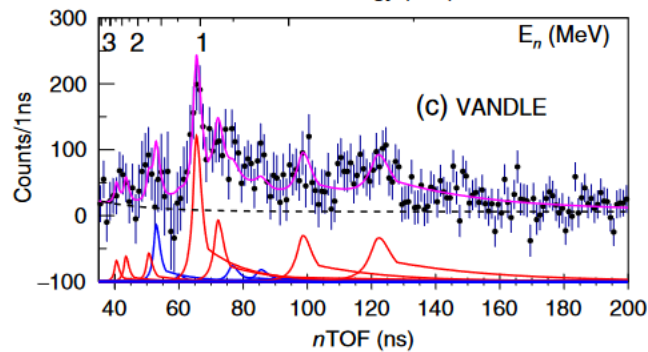
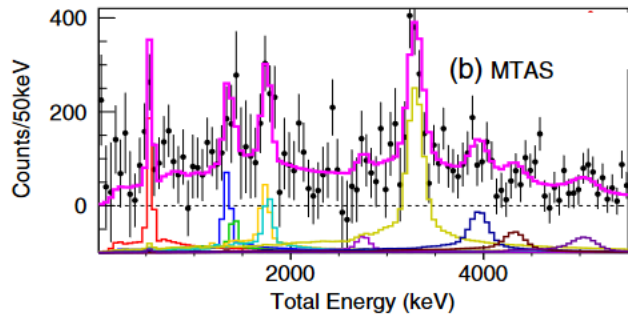
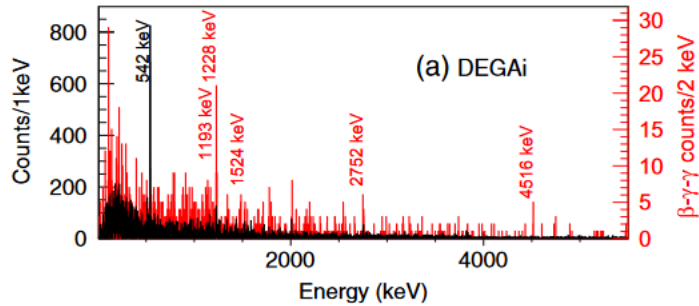
β decay of neutron-rich Cl isotopes, ^{45}Cl



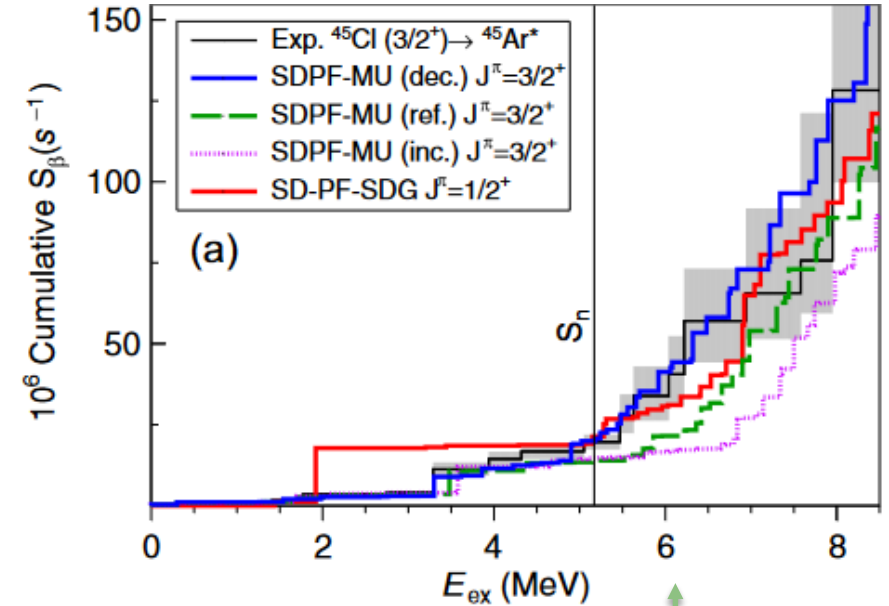
Complete spectroscopy performed at FRIB followed by β -decay of ^{45}Cl .



β decay of neutron-rich Cl isotopes, ^{45}Cl

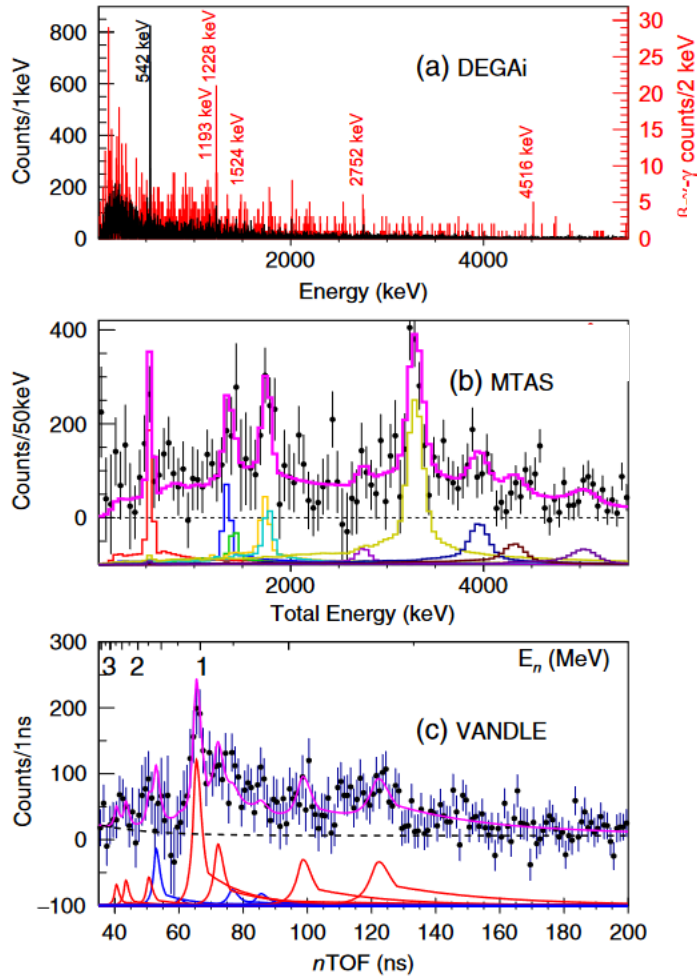


Complete spectroscopy performed at FRIB followed by β -decay of ^{45}Cl .

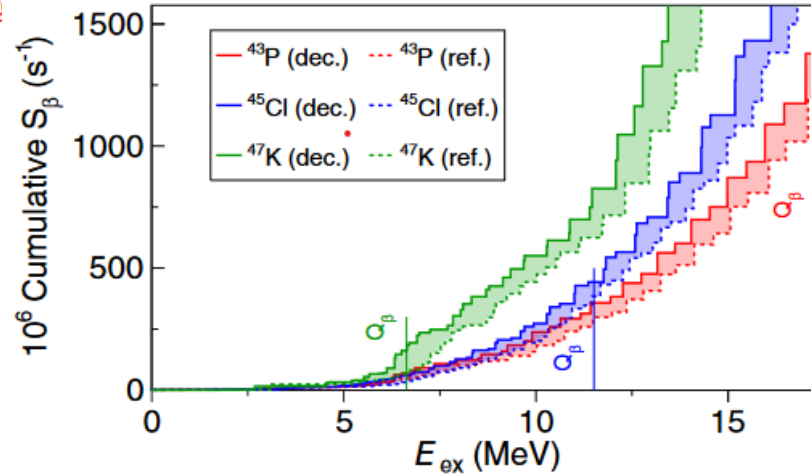


- Increased S_β above ^{45}Ar S_n was interpreted as the GT transition populating ^{45}Ar states with a proton excitation across $N=20$ shell gap
- Comparison of experimental S_β of ^{45}Cl to theoretical prediction with different models.

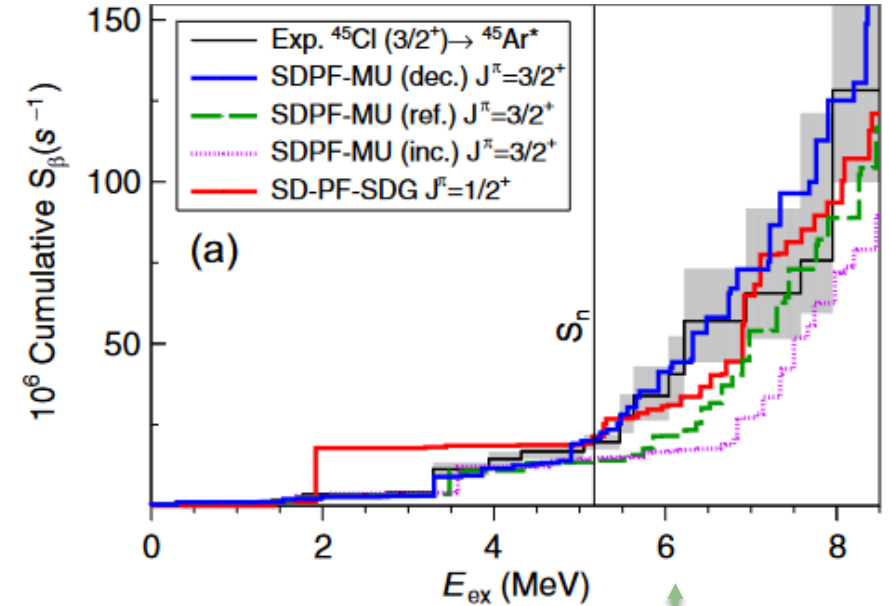
β decay of neutron-rich Cl isotopes, ^{45}Cl



Complete spectroscopy performed at FRIB followed by β -decay of ^{45}Cl .



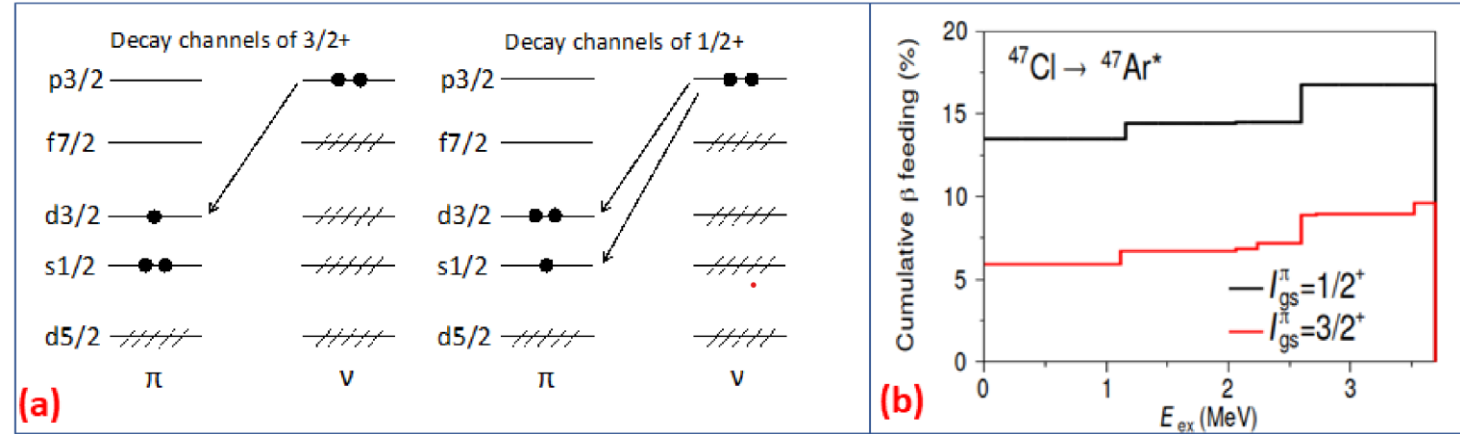
Cumulative S_β for odd-Z decays along $N=28$, calculated using a modified version of SDPF-MU* interaction.



- Increased S_β above ^{45}Ar S_n was interpreted as the GT transition populating ^{45}Ar states with a proton excitation across $N=20$ shell gap
- Comparison of experimental S_β of ^{45}Cl to theoretical prediction with different models.

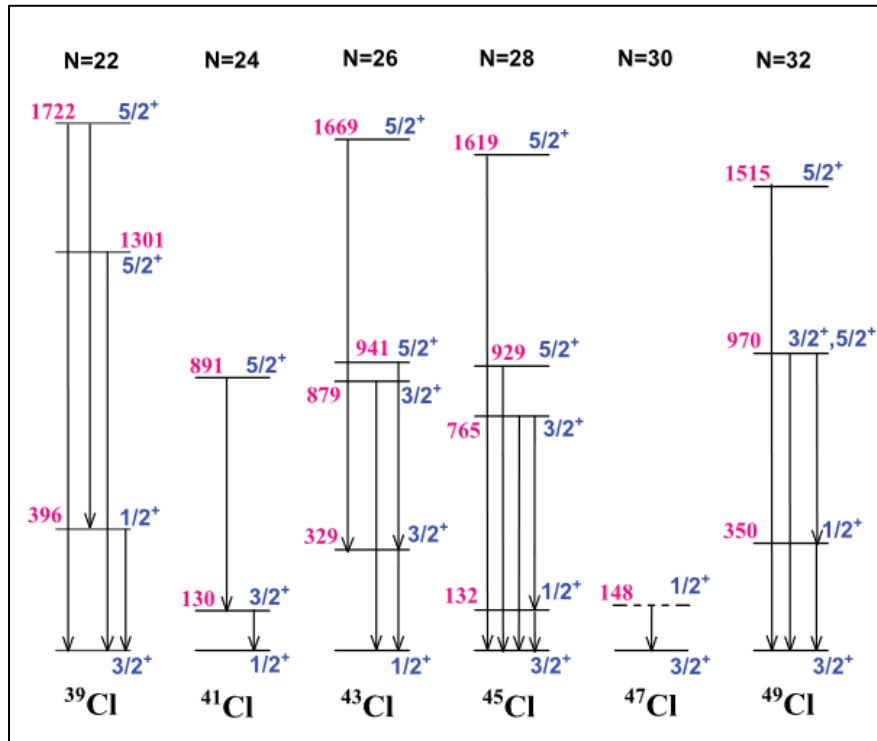
β decay of neutron-rich Cl isotopes, ^{47}Cl

- (a) Possible first-forbidden decay channel in the single-particle picture of ^{47}Cl .
- (b) Cumulative β -feeding probability of ^{47}Cl with SDPF-MU¹ shell-model interaction.



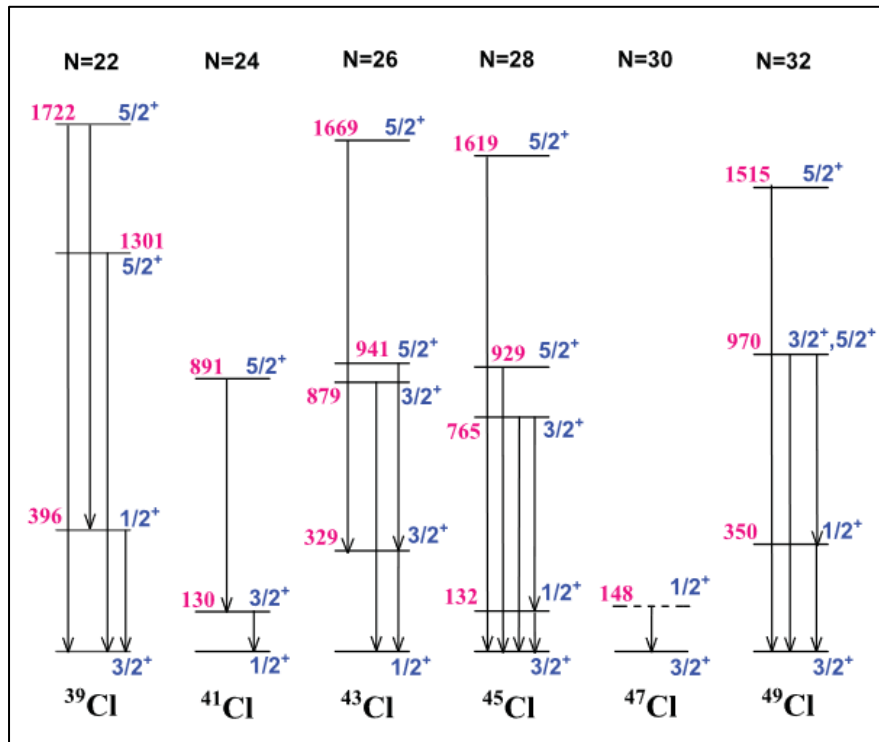
- Role of First Forbidden transitions in determining P_{xn} values and $T_{1/2}$ values.
- Understanding the delayed neutron spectrum and its relation to the B(GT) strength distribution.
- Understand the structure of the descendant nuclei.

Systematics of odd-mass Cl and K isotopes



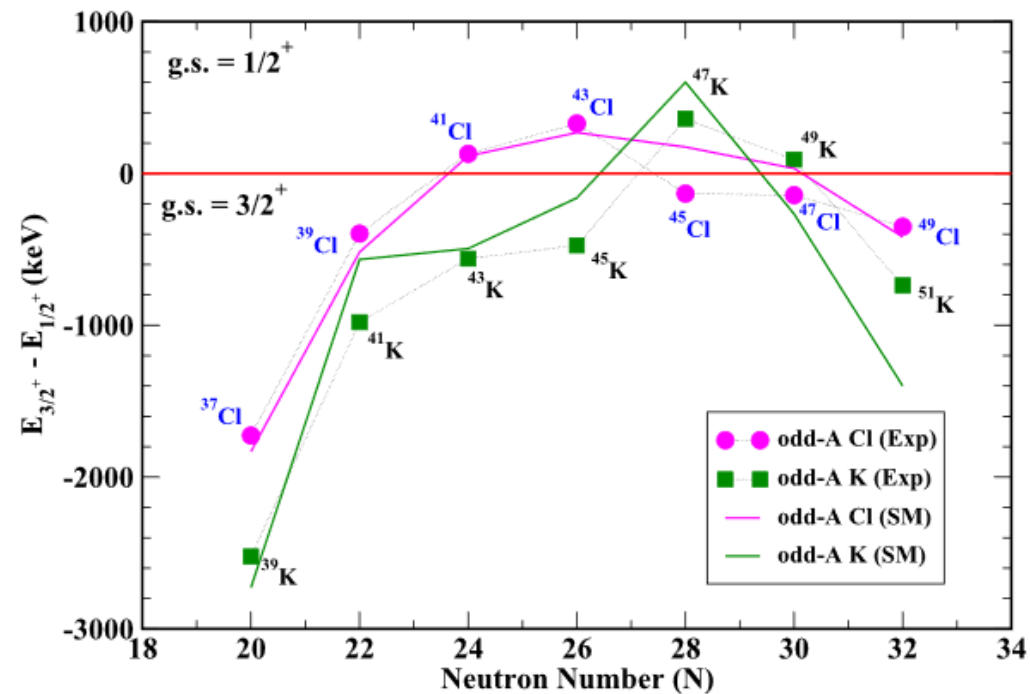
- Spin-parity assigned mainly following systematics, γ -ray decay pattern, β -decay, theory predictions.
- No direct measurements were conducted.

Systematics of odd-mass Cl and K isotopes



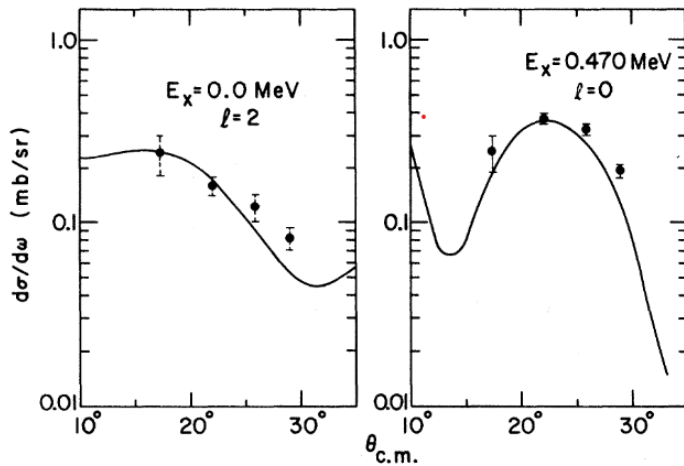
- Spin-parity assigned mainly following systematics, γ -ray decay pattern, β -decay, theory predictions.
- No direct measurements were conducted.

- Ground-state spin inversion between $3/2^+$ and $1/2^+$ in odd-mass K and Cl isotopes.
- Experimental energy differences compared with the shell model performed with the SD-PF-SDG^{*} interaction.



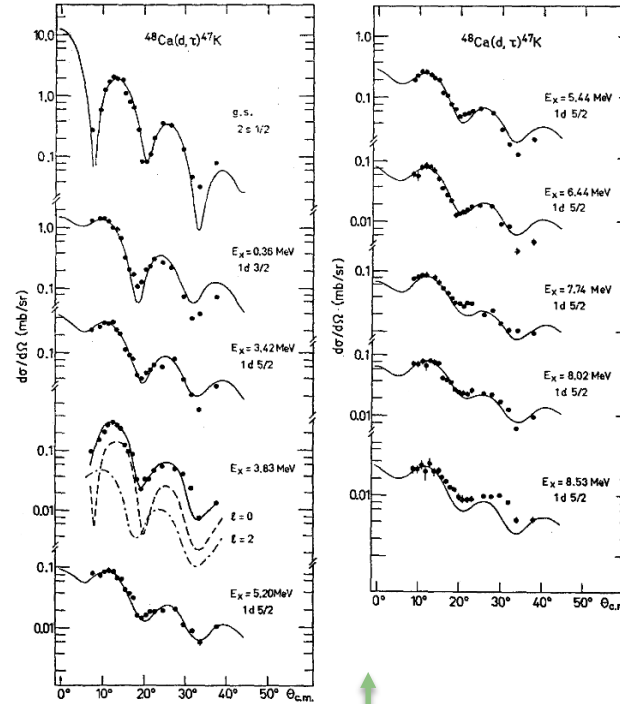
Particle-transfer reactions can provide guidance

J.L.Yntema *et al.*, Phys. Rev. C 4, 1621 (1971)



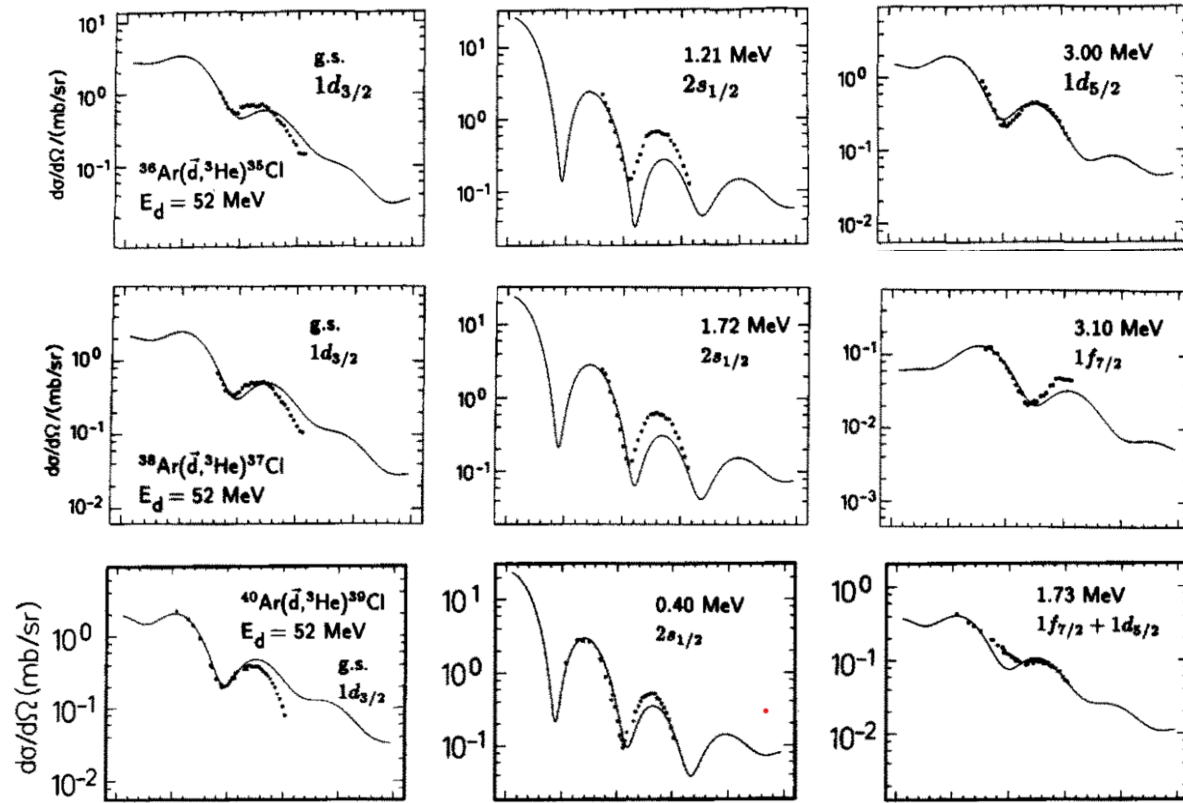
- $^{46}\text{Ca}(d,^3\text{He})^{45}\text{K}$ reaction to study ^{45}K .
- Ground-state configuration dominated by unpaired proton in $d_{3/2}$.

P.Doll *et al.*, Nucl. Phys. A 2, 210 (1976)



- $^{48}\text{Ca}(d,^3\text{He})^{47}\text{K}$ reaction to study ^{47}K .
- Ground-state configuration dominated by unpaired proton in $s_{1/2}$.

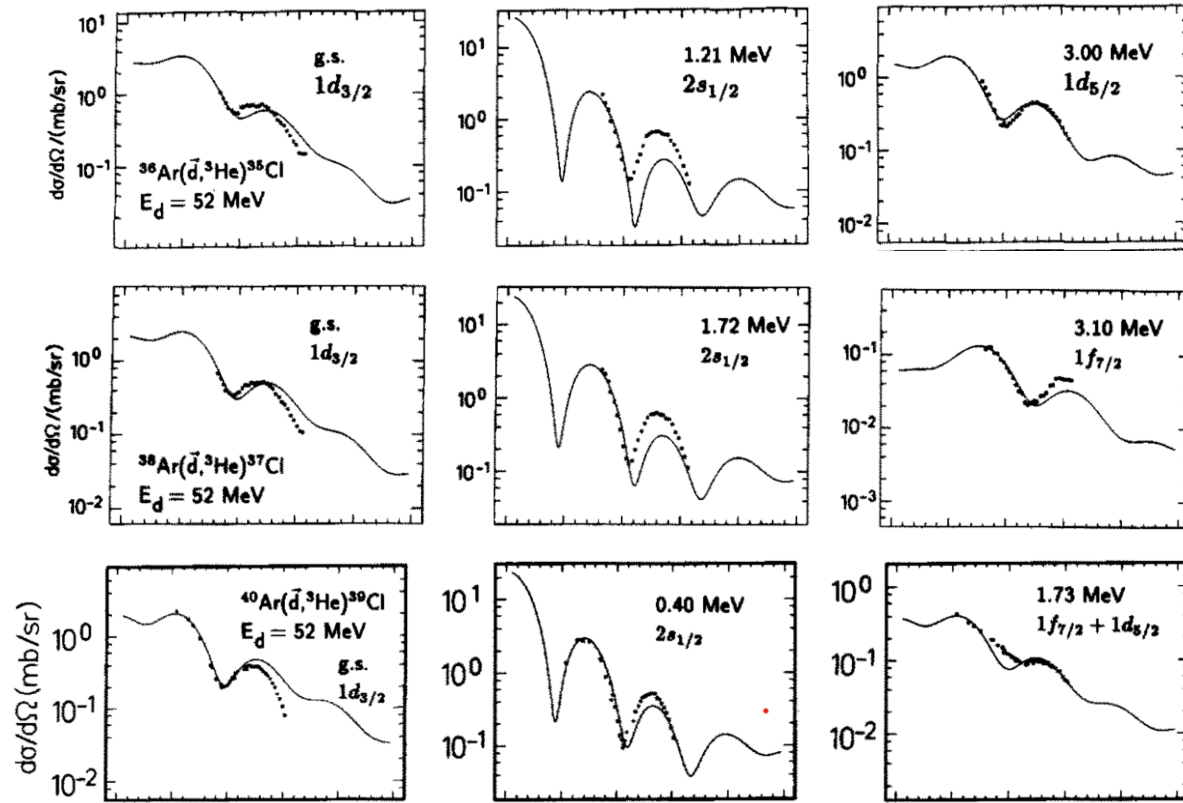
Particle-transfer reactions can provide guidance



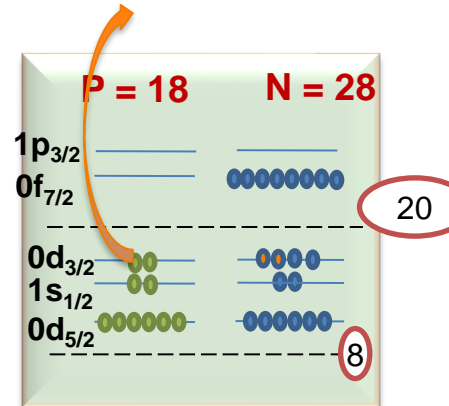
- No experimental data for higher masses available from direct reaction.
- Radioactive Ion (RI) beams can help.

- $^{36,38,40}\text{Ar}(d, ^3\text{He})^{35,37,39}\text{Cl}$ reactions provide measurement of proton pickup.
- Ground-state configuration dominated by unpaired proton in $d_{3/2}$.

Particle-transfer reactions can provide guidance



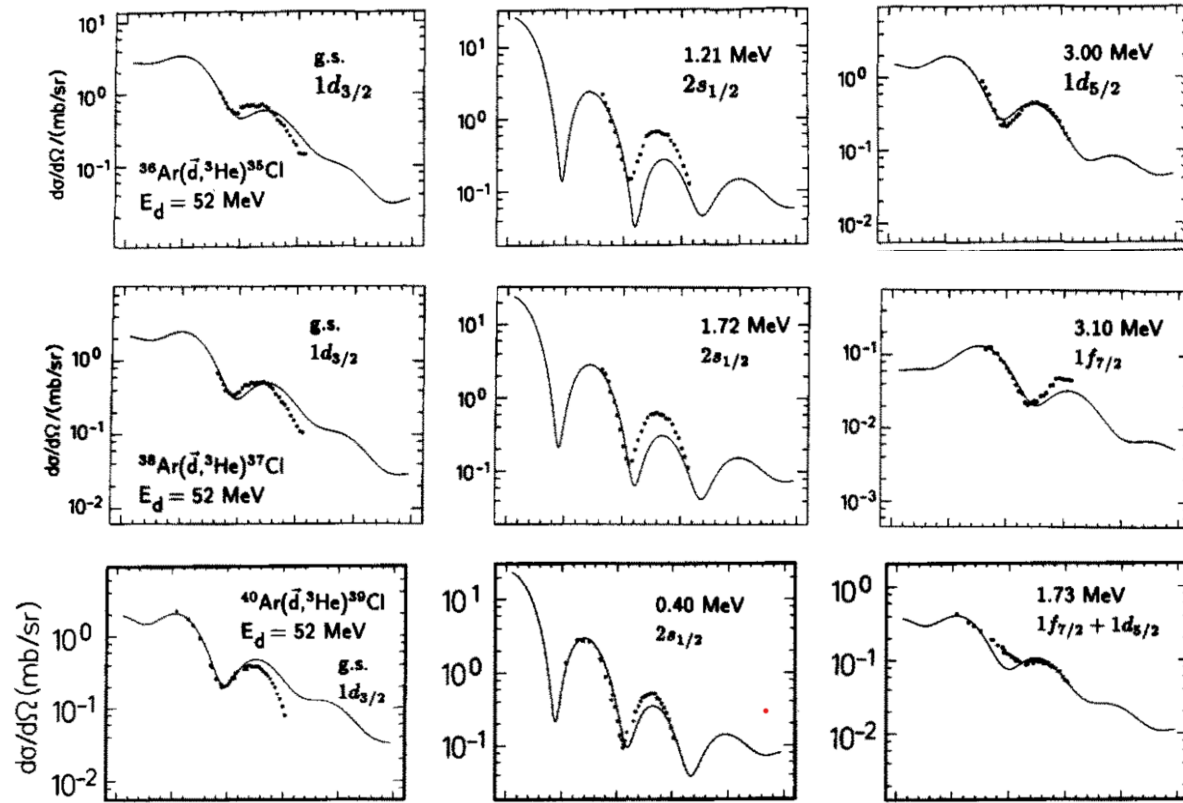
- Proton removal reactions can provide direct insight into the proton shell evolutions.



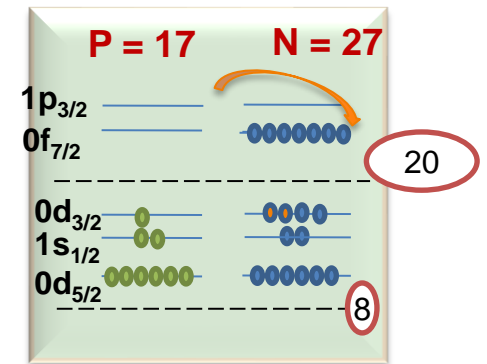
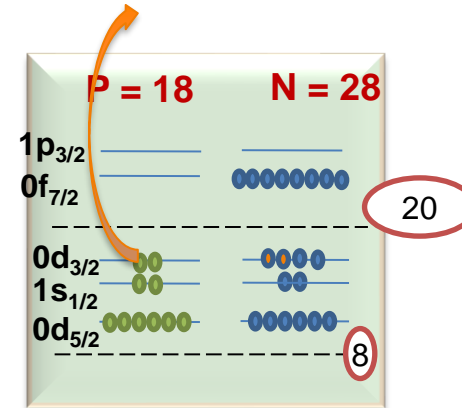
$^{46}\text{Ar}(d, ^3\text{He})^{45}\text{Cl}$ reaction to study the ground-state proton configuration of ^{45}Cl .

- $^{36,38,40}\text{Ar}(d, ^3\text{He})^{35,37,39}\text{Cl}$ reactions provide measurement of proton-hole states.
- Ground-state configuration dominated by unpaired proton in $d_{3/2}$.

Particle-transfer reactions can provide guidance



- Proton removal reactions can provide direct insight into the proton shell evolutions.
- For neutron shell evolutions, some best choices are neutron adding/removal reactions.



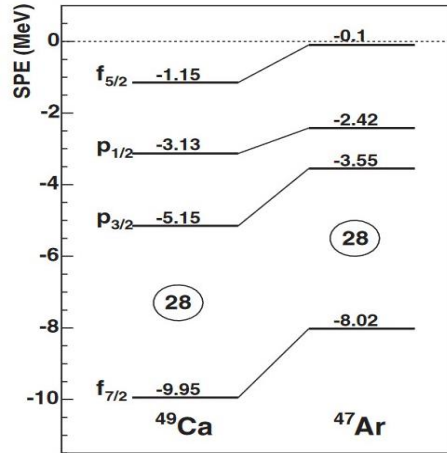
$^{46}\text{Ar}(d, ^3\text{He})^{45}\text{Cl}$ reaction to study the ground-state proton configuration of ^{45}Cl .

$^{44}\text{Cl}(d,p)^{45}\text{Cl}$ reaction to study the emptiness or fullness of the $f_{7/2}$, $p_{3/2}$, evolution of the fp-shell orbitals.

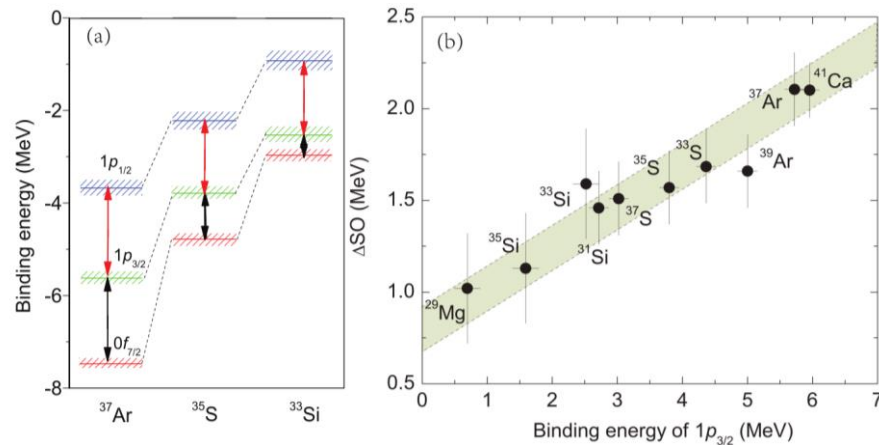
- $^{36,38,40}\text{Ar}(d, ^3\text{He})^{35,37,39}\text{Cl}$ reactions provide measurement of proton-hole states.
- Ground-state configuration dominated by unpaired proton in $d_{3/2}$.

N=28 shell gap migration via particle-transfer reactions

L. Gaudefroy et al., Phys. Rev. Lett. 97, 092501



- Evolution in SPE and spin-orbit (SO) splitting between $1p_{3/2}$ and $1p_{1/2}$ around N=28 isotones were studied.
- Systematics around N=20 was explored.
- Single nucleon transfer reaction is one of the best approaches.



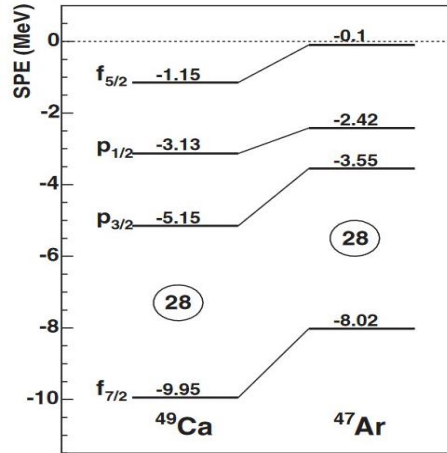
J. Chen et al., Phys. Lett. B 835, 138678 (2024)

*Y. Utsuno et al., Phys. Rev. C 86, 051301(R) (2012)

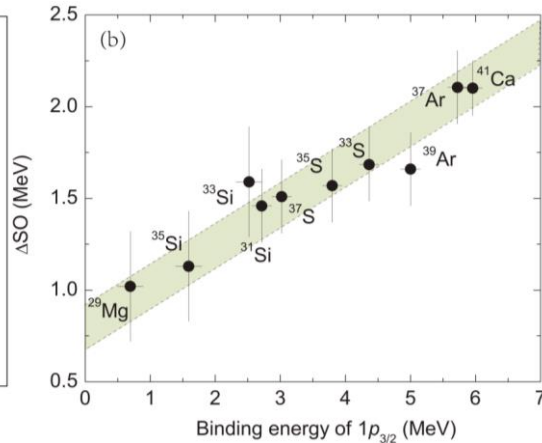
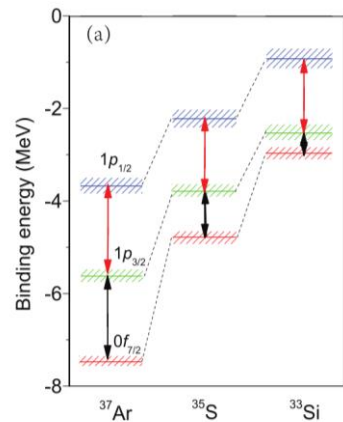


N=28 shell gap migration via particle-transfer reactions

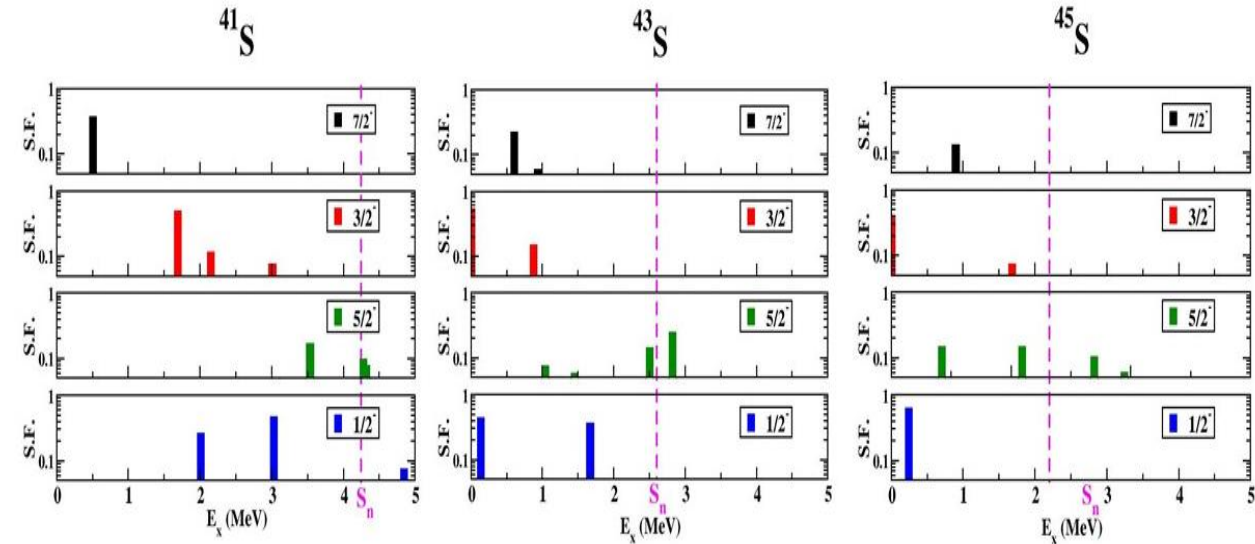
L. Gaudefroy et al., Phys. Rev. Lett. 97, 092501



- Evolution in SPE and spin-orbit (SO) splitting between $1p_{3/2}$ and $1p_{1/2}$ around N=28 isotones were studied.
- Systematics around N=20 was explored.
- Single nucleon transfer reaction is one of the best approaches.



J. Chen et al., Phys. Lett. B 835, 138678 (2024)

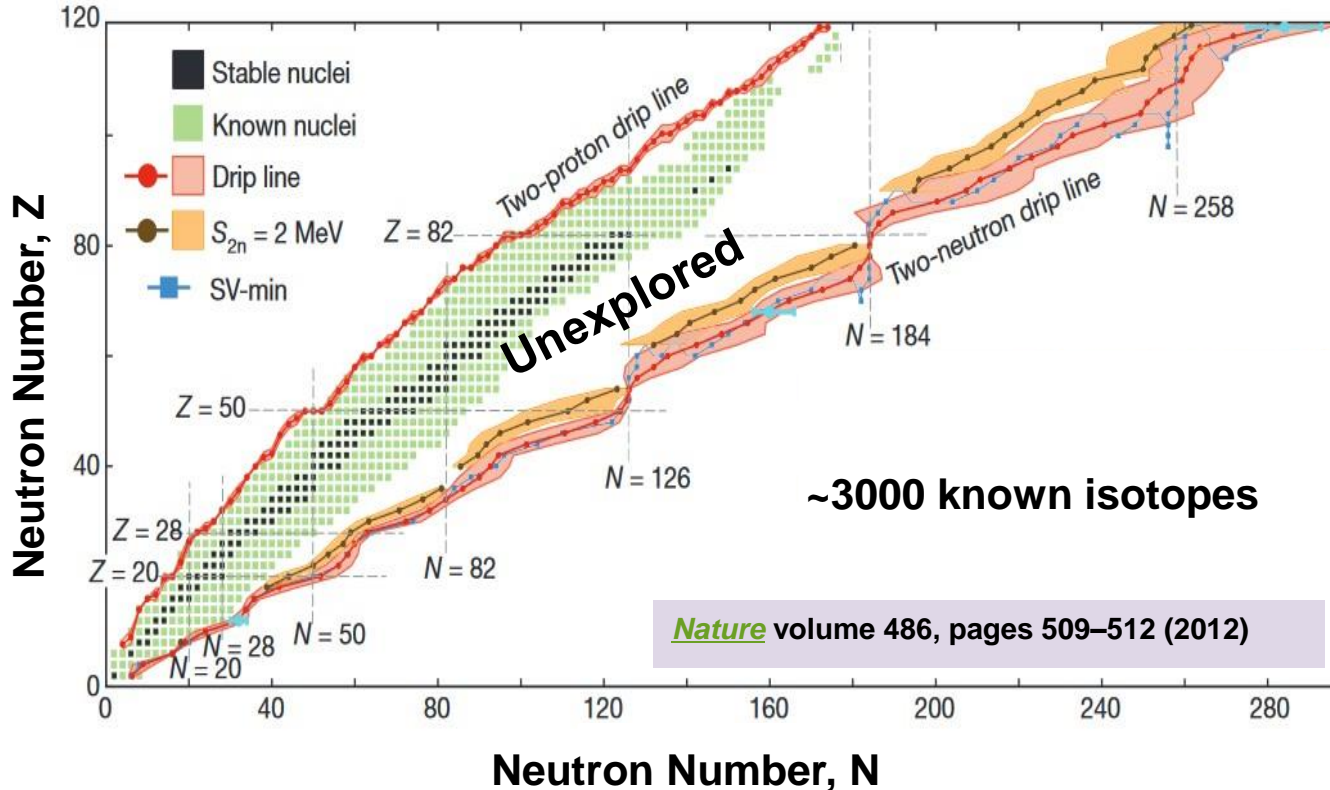


- S isotopes around $N=28$ are well known for their deformed nature.
- (d,p) , (d,t) reactions can extract single particle properties.
- Determine spin-orbit splitting from SPE of the fp -shell orbitals.
- Fragmentation of single particle strength.
- Energy, spectroscopic factors predicted with the SDPF-MU interaction*.

*Y. Utsuno et al., Phys. Rev. C 86, 051301(R) (2012)



Unlocking Potentials...



- Huge discovery potential with the rare isotope (RI) beams and state-of-arts detection systems.
- More exotic isotopes can be explored.
- Unconventional structural properties.
- Can provide crucial role in developing comprehensive models to track the structural trajectories from stable towards drip-line nuclei consistently.

Thank you

Sincere thanks to the collaborators.

**Work supported by the U.S. Department of Energy, Office of Science,
Office of Nuclear Physics, under Grant No DE-SC0020451 (FRIB).**



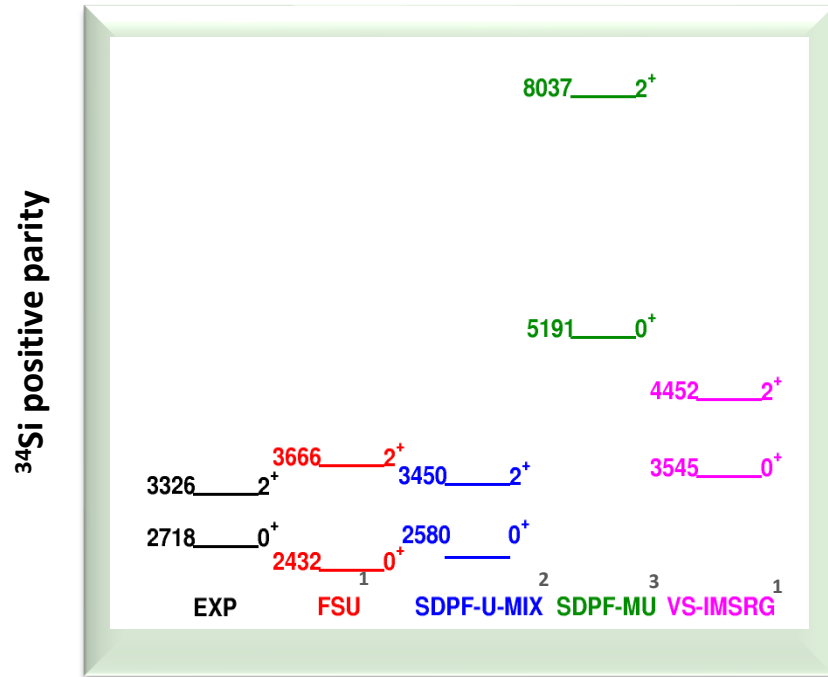
Back up slides



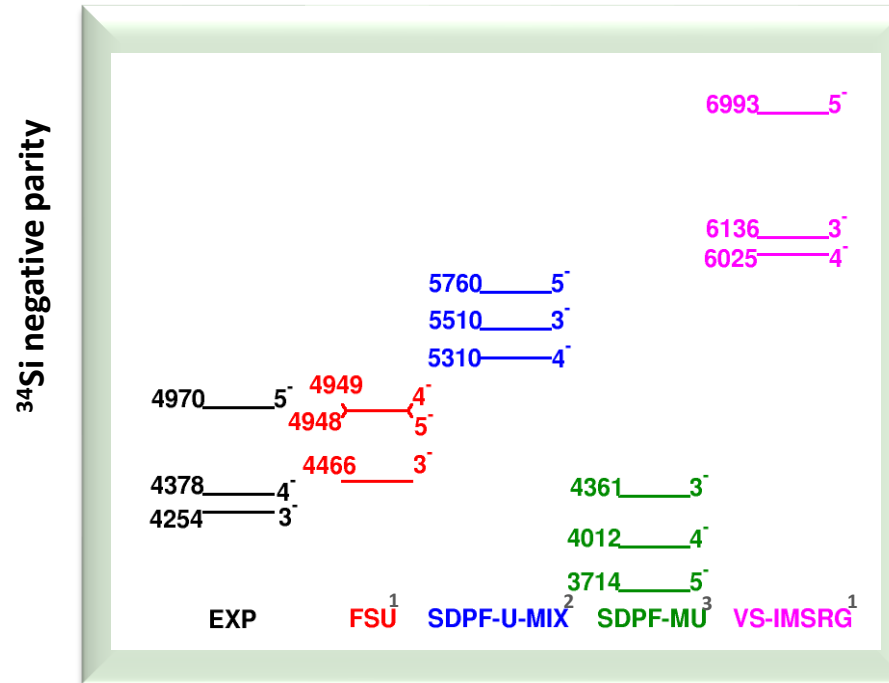
Type	L	$\Delta\pi$	Fermi ΔI	Gamow-Teller ΔI	Log ft
Superallowed	0	No	0	0	2.9-3.7
Allowed	0	No	0	0,1	4.4-6.0
1st Forbidden	1	Yes	0, 1	0, 1, 2	6-10
2nd Forbidden	2	Yes	1,2	1, 2, 3	10-13



^{34}Si : Transitional Nucleus along $N = 20$



- Compared the experimental levels with some modern theoretical models.
- SDPF-U-MIX, SDPF-MU, VS-IMSRG calculations consider mixing. FSU calculations do not consider any mixing in different types of excitations.
- FSU, SDPF-U-MIX and VS-IMSRG well predicts the first excited 0^+ and 2^+ with the $2\hbar\omega$ excitation.



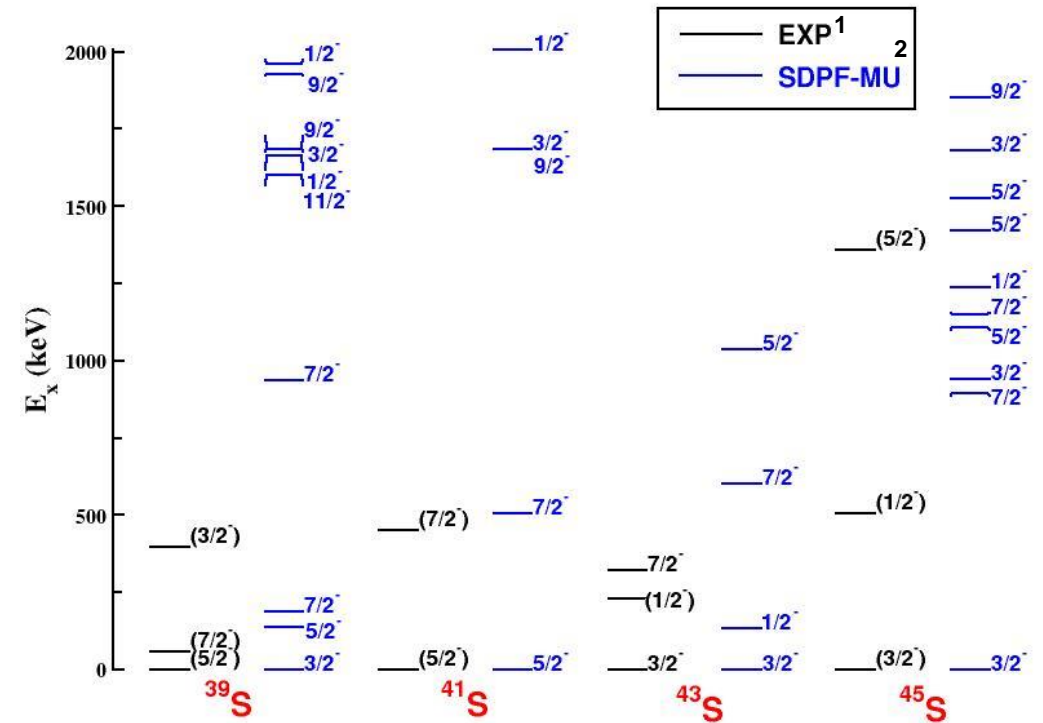
- The first negative parity 3^- , 4^- , 5^- states are dominated by the $1\hbar\omega$ excitation with the dominant configuration $(\nu d_{3/2})^1 \otimes (\nu f_{7/2})^1$
- All except for FSU interaction fail to predict opposite parity states.

Particle transfer reaction with SOLARIS at FRIB

Simultaneous (d, p) and (d, t) with $^{40,42}\text{S}$ beams (Accepted)

- S isotopes around $N=28$ are well known for their deformed nature.
- The advantage of simultaneous measurements is a reliable extraction of the effective single-particle energies (ESPE) of the neutron fp-shell orbitals.
- Determine spin-orbit splitting from ESPE of the fp-shell orbitals.
- Evolution of ESPEs
- Fragmentation of single particle strength.

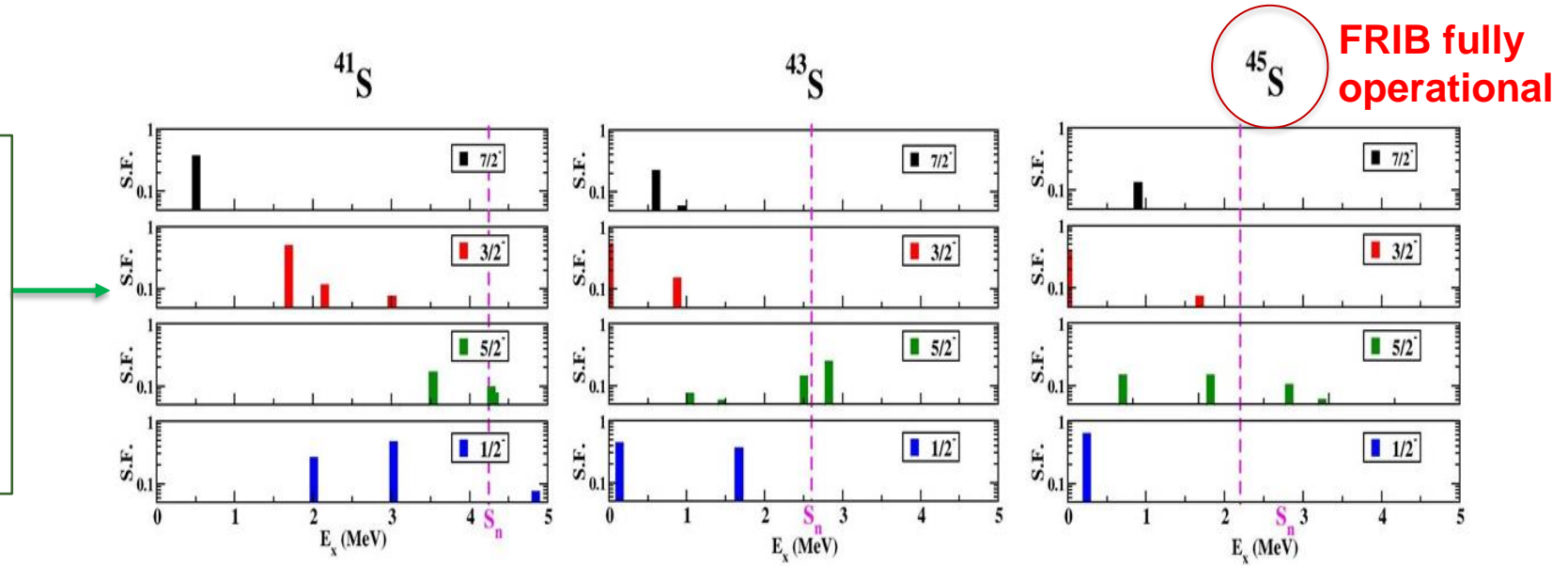
- Experimentally observed energy states compared with the predictions made by SDPF-MU interaction



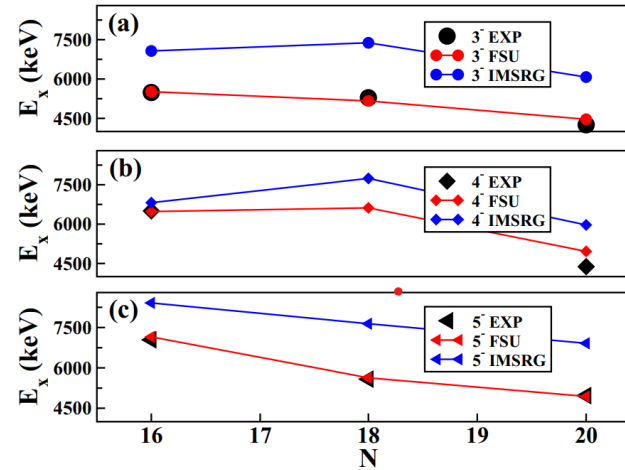
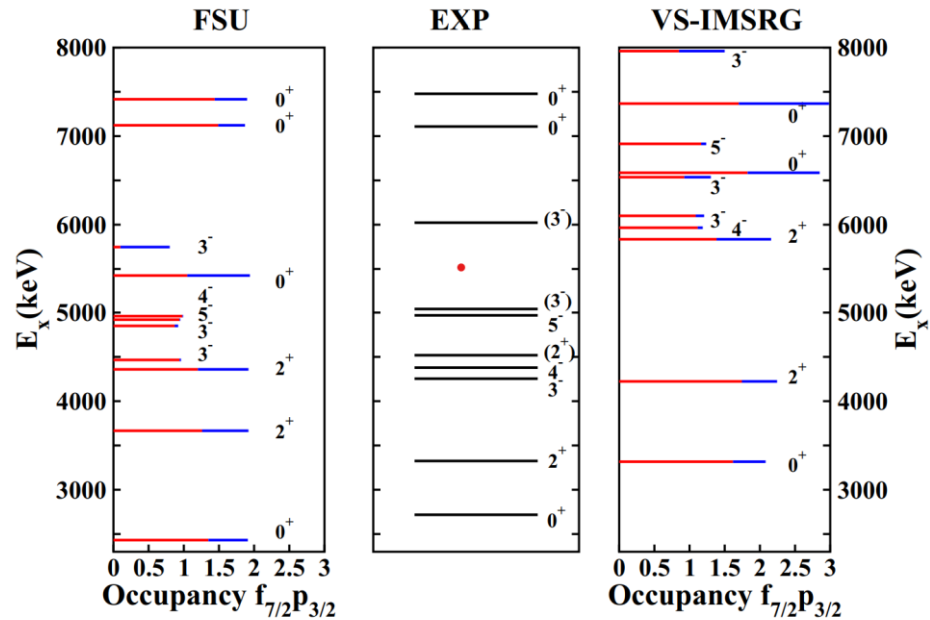
Particle transfer reaction with SOLARIS at FRIB

Simultaneous (d, p) and (d, t) with $^{40,42}\text{S}$ beams (Accepted)

- One neutron adding S.F. plotted for different energy levels of $^{41,43,45}\text{S}$ predicted with the SDPF-MU¹ shell-model interaction.
- Simultaneous (d, p) and (d, t) using SOLARIS at FRIB with $^{40,42}\text{S}$ beams.



^{34}Si Structure: Shell-model Predictions

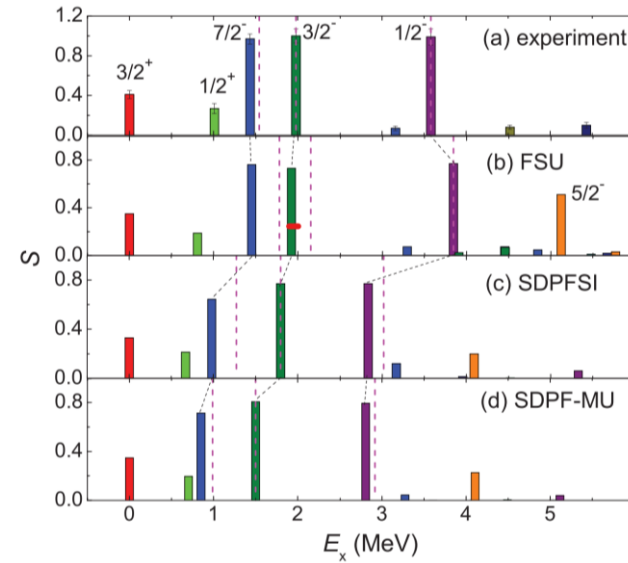
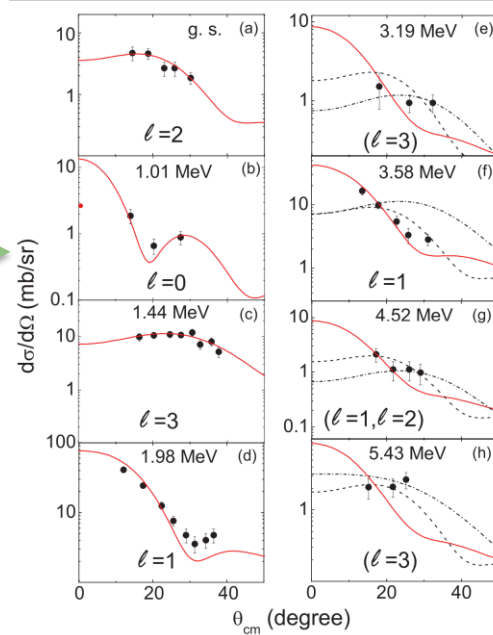


(a) ^{30}Si (b) ^{32}Si (c) ^{34}Si

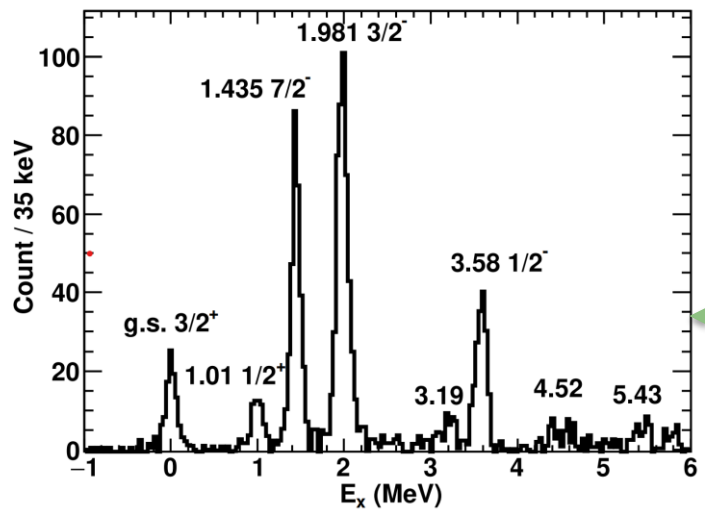
- Compared the experimental levels with two modern theoretical models.
- Lowest 3^- , 4^- , 5^- states are dominated by the $1\hbar\omega$ excitation with the dominant configuration $(\nu d_{3/2})^1 \otimes (\nu f_{7/2})^1$
- FSU successfully predicts systematics of $-ve$ parity even-mass Si isotopes.

Evolution of SPE and spin-orbit spacing

Differential cross sections for low-lying states of ^{33}Si . DWBA calculations are plotted as solid red lines

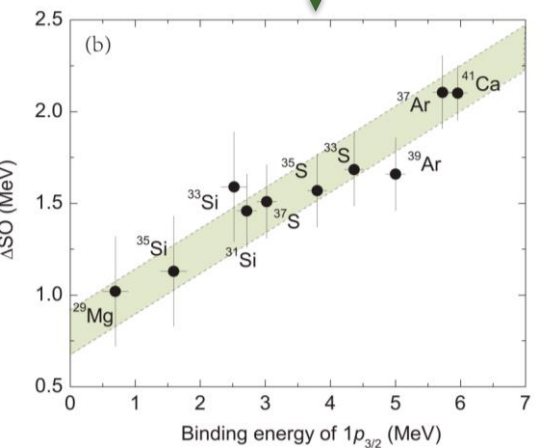
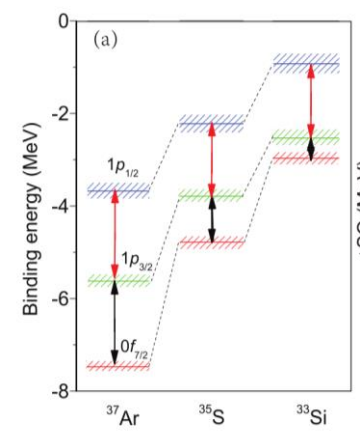


Spectroscopic factors compared with predictions made by shell-model calculations

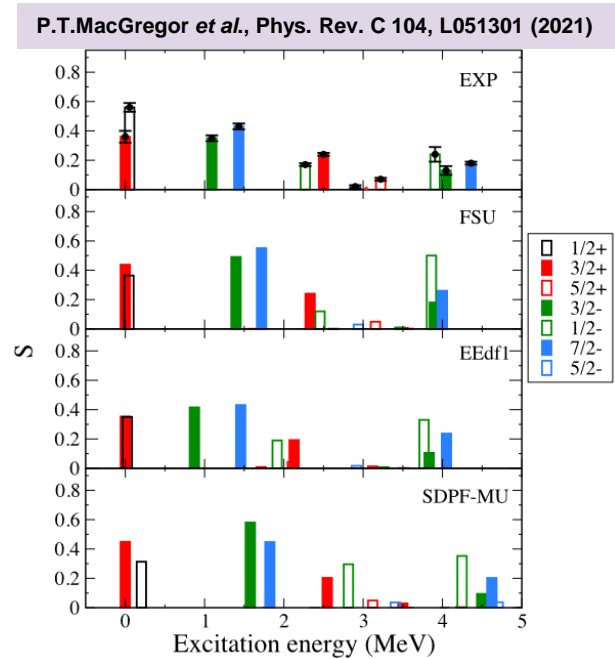


excitation-energy spectrum for states in ^{33}Si populated via the $^{32}\text{Si}(d, p)$ reaction

Evolution of SPE



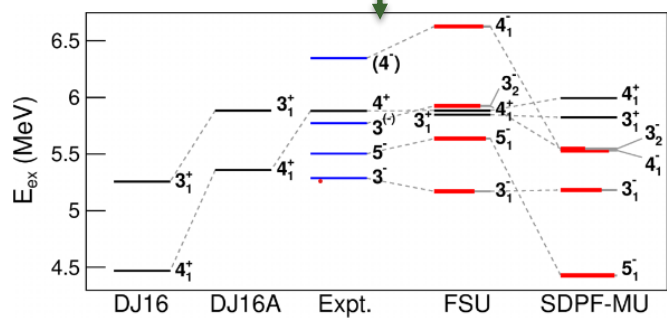
Interpretation of the experimental observables



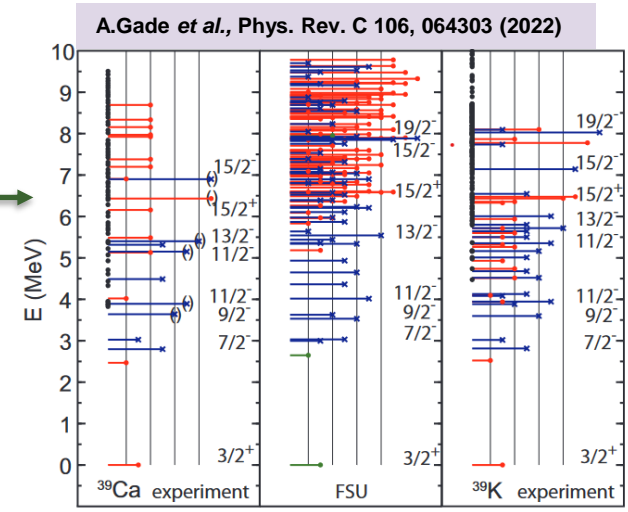
- States populated in ^{29}Mg via (d, p) reaction.
- Opposite-parity states provide test to the models.

- States of mirror nuclei ^{39}Ca and ^{39}K studied via γ -ray spectroscopy.
- Opposite-parity states provide test to the newly developed interaction.

States of ^{32}Si identified via γ -ray spectroscopy were compared with models.



J. Williams *et al.*, Phys. Rev. C 108, L051305 (2023)



Experimental $B(E2; 3/2^- \rightarrow J^\pi)$ values of ^{29}Ne compared with different models.

